
Active Slices for Sliced Stein Discrepancy

Wenbo Gong¹ Kaibo Zhang¹ Yingzhen Li² José Miguel Hernández-Lobato¹

Abstract

Sliced Stein discrepancy (SSD) and its kernelized variants have demonstrated promising successes in goodness-of-fit tests and model learning in high dimensions. Despite their theoretical elegance, their empirical performance depends crucially on the search of optimal slicing directions to discriminate between two distributions. Unfortunately, previous gradient-based optimisation approaches for this task return sub-optimal results: they are computationally expensive, sensitive to initialization, and they lack theoretical guarantees for convergence. We address these issues in two steps. First, we provide theoretical results stating that the requirement of using optimal slicing directions in the kernelized version of SSD can be relaxed, validating the resulting discrepancy with *finite* random slicing directions. Second, given that good slicing directions are crucial for practical performance, we propose a fast algorithm for finding such slicing directions based on ideas of active sub-space construction and spectral decomposition. Experiments on goodness-of-fit tests and model learning show that our approach achieves both improved performance and faster convergence. Especially, we demonstrate a 14-80x speed-up in goodness-of-fit tests when comparing with gradient-based alternatives.

1. Introduction

Discrepancy measures between two distributions are critical tools in modern statistical machine learning. Among them, *Stein discrepancy* (SD) and its kernelized version, kernelized Stein discrepancy (KSD), have been extensively used for *goodness-of-fit* (GOF) testing (Liu et al., 2016;

Chwialkowski et al., 2016; Huggins & Mackey, 2018; Jitkritum et al., 2017; Gorham & Mackey, 2017) and model learning (Liu & Wang, 2016; Pu et al., 2017; Hu et al., 2018; Grathwohl et al., 2020). Despite their recent success, applications of Stein discrepancies to high-dimensional distribution testing and learning remains an unsolved challenge.

These “curse of dimensionality” issues have been recently addressed by the newly proposed Sliced Stein discrepancy (SSD) (Gong et al., 2021) and its kernelized variants (i.e. SKSD), which have demonstrated promising results in both high dimensional GOF tests and model learning. They work by first projecting the score function and the test inputs across two slice directions r and g_r and then comparing the two distributions using the resulting one dimensional slices. The performance of SSD and SKSD crucially depends on choosing slicing directions that are highly discriminative. Indeed, Gong et al. (2021) showed that such discrepancy can still be valid despite the information loss caused by the projections if *optimal slices* are used. These are directions along which the two distributions differ the most. Unfortunately, gradient-based optimization for searching such optimal slices often suffers from slow convergence and sub-optimal solutions. In practice, many gradient updates may be required to obtain a reasonable set of slice directions (Gong et al., 2021).

We aim to tackle the above practical challenges by proposing an efficient algorithm to find *good* slice directions with statistical guarantees. Our contributions are as follows:

- We propose a computationally efficient variant of SKSD using a *finite number of random slices*. This relaxes the restrictive constraint of having to use *optimal* slices, with the consequence that convergence during optimisation to a global optimum is no longer required.
- Given that *good* slices are still preferred in practice, we propose surrogate optimization tasks to find such directions. These are called *active slices* and have analytic solutions that can be computed very efficiently.
- Experiments on GOF test benchmarks (including testing on restricted Boltzmann machines) show that our algorithm outperforms alternative gradient-based approaches while achieving at least a 14x speed-up.
- In the task of learning high dimensional *independent component analysis* (ICA) models (Comon, 1994), our

¹Department of Engineering, University of Cambridge, Cambridge, United Kingdom ²Department of Computing, Imperial College London, London, United Kingdom. Correspondence to: Wenbo Gong <wg242@cam.ac.uk>, José Miguel Hernández-Lobato <jmh233@cam.ac.uk>.

algorithm converges much faster and to significantly better solutions than other baselines.

Road map: First, we give a brief background for SD , SSD and its relevant variants (Section 2). Next, we show how to relax the previously required optimality constraints to using finite random slice directions (Section 3.1). We then motivate the surrogate optimisation tasks for finding good slices by showing the relationship between $SKSD$ and SSD (Section 3.2). Lastly, we propose algorithms to find active slices (Sections 4, 5, 6), and demonstrate the efficacy of our proposal in the experiments (Section 7). Assumptions and proofs of theoretical results as well as the experimental settings can be found in the appendix.

2. Background

For a distributions p on $\mathcal{X} \subset \mathbb{R}^D$ with differentiable density, we define its score function as $\mathbf{s}_p(\mathbf{x}) = \nabla_{\mathbf{x}} \log p(\mathbf{x})$. We also define the Stein operator \mathcal{A}_p for distribution p as

$$\mathcal{A}_p \mathbf{f}(\mathbf{x}) = \mathbf{s}_p(\mathbf{x})^T \mathbf{f}(\mathbf{x}) + \nabla_{\mathbf{x}}^T \mathbf{f}(\mathbf{x}), \quad (1)$$

where $\mathbf{f} : \mathcal{X} \rightarrow \mathbb{R}^D$ is a test function. Then the *Stein discrepancy* (SD) (Gorham & Mackey, 2015) between two distributions p, q with differentiable densities on \mathcal{X} is

$$D_{SD}(q, p) = \sup_{\mathbf{f} \in \mathcal{F}_q} \mathbb{E}_q[\mathcal{A}_p \mathbf{f}(\mathbf{x})], \quad (2)$$

where \mathcal{F}_q is the Stein’s class of q that contains test functions satisfying $\mathbb{E}_q[\mathcal{A}_q \mathbf{f}(\mathbf{x})] = 0$ (also see Definition B.2 in appendix B). The supremum can be obtained by choosing $\mathbf{f}^* \propto \mathbf{s}_p(\mathbf{x}) - \mathbf{s}_q(\mathbf{x})$ if \mathcal{F}_q is rich (Hu et al., 2018).

Chwialkowski et al. (2016); Liu et al. (2016) further restricts the test function space \mathcal{F}_q to be a unit ball in an RKHS induced by a c_0 -universal kernel $k : \mathcal{X} \times \mathcal{X} \rightarrow \mathbb{R}$. This results in the *kernelized Stein discrepancy* (KSD):

$$D^2(q, p) = \left(\sup_{\mathbf{f} \in \mathcal{H}_k, \|\mathbf{f}\|_{\mathcal{H}_k} \leq 1} \mathbb{E}_q[\mathcal{A}_p \mathbf{f}(\mathbf{x})] \right)^2 = \|\mathbb{E}_q[\mathbf{s}_p(\mathbf{x})k(\mathbf{x}, \cdot) + \nabla_{\mathbf{x}} k(\mathbf{x}, \cdot)]\|_{\mathcal{H}_k}^2, \quad (3)$$

where \mathcal{H}_k is the k induced RKHS with norm $\|\cdot\|_{\mathcal{H}_k}$.

2.1. Sliced kernelized Stein discrepancy

Despite the theoretical elegance of KSD , it often suffers from the curse-of-dimensionality in practice. To address this issue, Gong et al. (2021) proposed a divergence family called *sliced Stein discrepancy* (SSD). The key idea is to compare the distributions on their one dimensional slices by projecting the score \mathbf{s}_p and test input \mathbf{x} with two directions \mathbf{r} and its corresponding \mathbf{g}_r , respectively. Readers are referred to appendix C for details. The loss of information due

to this projection operation can be mitigated by using an orthogonal basis for \mathbf{r} along with the corresponding \mathbf{g}_r directions with largest discriminative power (Gong et al., 2021). The resulting valid discrepancy is called *maxSSD-g*, which uses a set of orthogonal basis $\mathbf{r} \in O_r$ and their corresponding optimal \mathbf{g}_r directions:

$$S_{\max_{g_r}}(q, p) = \sum_{\mathbf{r} \in O_r} \sup_{\substack{h_{r g_r} \in \mathcal{F}_q \\ \mathbf{g}_r \in \mathbb{S}^{D-1}}} \mathbb{E}_q[s_p^r(\mathbf{x})h_{r g_r}(\mathbf{x}^T \mathbf{g}_r) + \mathbf{r}^T \mathbf{g}_r \nabla_{\mathbf{x}^T \mathbf{g}_r} h_{r g_r}(\mathbf{x}^T \mathbf{g}_r)], \quad (4)$$

where $h_{r g_r} : \mathcal{K} \subseteq \mathbb{R} \rightarrow \mathbb{R}$ is the test function, \mathbb{S}^{D-1} is the D -dimensional unit sphere and $s_p^r(\mathbf{x}) = \mathbf{s}_p(\mathbf{x})^T \mathbf{r}$ is the projected score function. Under certain scenarios (Gong et al., 2021), i.e. GOF test, one can further improve the performance of *maxSSD-g* by replacing $\sum_{\mathbf{r} \in O_r}$ with $\sup_{\mathbf{r} \in \mathbb{S}^{D-1}}$ in Eq.4, resulting in another variant called *maxSSD-rg*. This increment in performance is due to the higher discriminative power that is obtained by using the optimal \mathbf{r} slice.

Gong et al. (2021) further proposed kernelized variants to address the intractability issue of the optimal test function $h_{r g_r}^*$ by letting \mathcal{F}_q to be in a unit ball of an RKHS induced by a c_0 -universal kernel $k_{r g_r}$. With

$$\xi_{p, r, g_r}(\mathbf{x}, \cdot) = s_p^r(\mathbf{x})k_{r g_r}(\mathbf{x}^T \mathbf{g}_r, \cdot) + \mathbf{r}^T \mathbf{g}_r \nabla_{\mathbf{x}^T \mathbf{g}_r} k_{r g_r}(\mathbf{x}^T \mathbf{g}_r, \cdot), \quad (5)$$

the *maxSKSD-g* (the kernelized version of *maxSSD-g*) is

$$SK_{\max_{g_r}}(q, p) = \sum_{\mathbf{r} \in O_r} \sup_{\mathbf{g}_r \in \mathbb{S}^{D-1}} \|\mathbb{E}_q[\xi_{p, r, g_r}(\mathbf{x})]\|_{\mathcal{H}_{r g_r}}^2, \quad (6)$$

where $\mathcal{H}_{r g_r}$ is the RKHS induced by $k_{r g_r}$ with the associated norm $\|\cdot\|_{\mathcal{H}_{r g_r}}$. Similarly, a kernelized version of *maxSSD-rg*, denoted by *maxSKSD-rg* ($SK_{\max_{r g_r}}$), is obtained by replacing $\sum_{\mathbf{r} \in O_r}$ with $\sup_{\mathbf{r} \in \mathbb{S}^{D-1}}$ in Eq.6.

Despite having an analytic form for the optimal test function, the practical challenge of computing the kernelized SSD variants is the computation of the optimal slice directions \mathbf{r} and \mathbf{g}_r . Gradient-based optimization (Gong et al., 2021) for such computation suffers from slow convergence; even worse, it is sensitive to initialization and returns sub-optimal solutions only. In such case it is unclear whether the resulting discrepancy is still valid, making the correctness of GOF test unverified. Therefore the first important question to ask is: are the optimality of slices a necessary condition for discrepancy validity? Remarkably, we show that the answer is **No** with mild assumptions on the kernel.

To simplify the theoretical analysis we need to avoid direct supremum computation for \mathbf{r} and \mathbf{g}_r . Thus, we define *SSD-g* (*SKSD-g* resp.) as Eq.4 (Eq.6 resp.) with a *given* \mathbf{g}_r instead of $\sup_{\mathbf{g}_r}$. We use S_{g_r} and SK_{g_r} to represent *SSD-g* and *SKSD-g*, respectively. If \mathbf{r} is also given, we define $S_{r g_r}$.

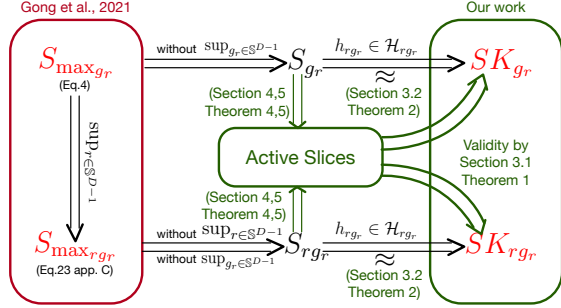


Figure 1. The relationship between different SSD discrepancies, where green texts indicate our contributions, red symbols indicate valid discrepancies and \mathcal{H}_{r, g_r} is the RKHS induced by kernel k_{r, g_r} .

as S_{g_r} without $\sum_{r \in O_r}$ and SK_{r, g_r} as $\|\mathbb{E}_q[\xi_{p, r, g_r}(\mathbf{x})]\|_{\mathcal{H}_{r, g_r}}^2$. They are called *SSD-rg* and *SKSD-rg*, respectively. Having set-up these notations, we visualize the structure of our paper in Figure 1.

3. Relaxing constraints for the SKSD family

3.1. Is optimality necessary for validity?

As mentioned before, the discrepancy validity of max SKSD requires the optimality of slice directions, which restricts its application in practice. In the following, we show that these restrictions can be much relaxed with mild assumptions on the kernel. All proofs can be found in Appendix E.

The key idea is to use kernels such that the corresponding term SK_{r, g_r} is *real analytic* w.r.t. both \mathbf{r} and \mathbf{g}_r . A nice property of any real analytic function is that, unless it is a constant function, otherwise the set of its roots has zero Lebesgue measure. This means the possible valid slices are almost everywhere in \mathbb{R}^D , giving us huge freedom to choose slices without worrying about violating validity.

Theorem 1 (Conditions for valid slices). *Assuming assumptions 1-4, 7 and 8 in Appendix B, let $\mathbf{g}_r \sim \eta_g$ for each $\mathbf{r} \sim \eta_r$, where η_g, η_r are distributions on \mathbb{R}^D with a density, then $SK_{r, g_r}(q, p) = 0$ iff. $p = q$ almost surely.*

The above theorem tells us that a *finite* number of *random* slices is enough to make SK_{r, g_r} valid without the need of using optimal slices (c.f. $SK_{\max_{r, g_r}}$). In practice, we often consider $\mathbf{r}, \mathbf{g}_r \in \mathbb{S}^{D-1}$ instead of \mathbb{R}^D . Fortunately, one can easily transform arbitrary slices to \mathbb{S}^{D-1} without violating the validity. For any \mathbf{r}, \mathbf{g}_r , we (i) add Gaussian noises to them, and (2) re-normalize the noisy \mathbf{r}, \mathbf{g}_r to unit vectors. We refer to corollary 6.1 in appendix E.1 for details.

3.2. Relationship between SSD and SKSD

Theorem 1 allows us to use random slices. However, it is still beneficial to find good ones in practice. Unfortunately, SK_{r, g_r} is not a suitable objective for finding good slice directions. This is because, unlike the test function in a general function space ($h_{r, g_r} \in \mathcal{F}_q$), the optimal kernel test function ($\mathbb{E}_q[\xi_{p, r, g_r}(\mathbf{x}, \cdot)]$) can not be easily analyzed for finding good slices due to its restriction in RKHS.

Instead, we propose to use S_g (or S_{r, g_r}) as the optimization objective. To justify S_{r, g_r} as a good replacement for SK_{g_r} , we show that SK_{r, g_r} approximates S_{r, g_r} arbitrarily well if the corresponding RKHS of the chosen kernel is dense in continuous function space. Similar results for $SK_g \approx S_g$ can be derived accordingly.

Theorem 2 ($SK_{r, g_r} \approx S_{r, g_r}$). *Assume assumptions 1-4 and 7. Given \mathbf{r} and \mathbf{g}_r , $\forall \epsilon > 0$ there exists a constant C such that*

$$0 \leq S_{r, g_r} - SK_{r, g_r} < C\epsilon.$$

The proof involves the optimal test function h_{r, g_r}^* for S_{r, g_r} , whose analytic form is in Proposition 3 of appendix E.2.

As S_{r, g_r} approximates SK_{r, g_r} arbitrary well, the hope is that good slices for S_{r, g_r} also correspond to good slices for SK_{r, g_r} in practice. Therefore in the next section we focus on analyzing S_{r, g_r} instead to propose an efficient algorithm for finding good slices.

4. Active slice direction \mathbf{g}

Finding good slices involves alternating maximization of \mathbf{r} and \mathbf{g}_r . To simplify the analysis, we focus on good directions \mathbf{g}_r given fixed \mathbf{r} , e.g. the orthogonal basis $\mathbf{r} \in O_r$ for now. Finding good \mathbf{g}_r is achieved in two steps: (i) Construct an equivalent minimization problem, called *controlled approximation*, to the maximization of S_{g_r} w.r.t \mathbf{g}_r ; (ii) Establish an upper-bound of the controlled approximation objective such that its minimizer is analytic. We name the resulting \mathbf{g}_r as *active slices*. All proofs can be found in appendix F.

4.1. Controlled Approximation

To start with, we need an upper bound for S_{g_r} so that we can transform the maximization of S_{g_r} into the minimization of their gap. Hence, we propose a generalization of SD (Eq.2) called *projected Stein discrepancy* (PSD):

$$\text{PSD}(q, p; O_r) = \sum_{\mathbf{r} \in O_r} \sup_{f_r \in \mathcal{F}_q} \mathbb{E}_q[s_p^T(\mathbf{x})f_r(\mathbf{x}) + \mathbf{r}^T \nabla_{\mathbf{x}} f_r(\mathbf{x})] \quad (7)$$

where $f_r : \mathcal{X} \subseteq \mathbb{R}^D \rightarrow \mathbb{R}$. SD is a special case of PSD by setting O_r as identity matrix \mathbf{I} . In proposition 4 of appendix

F.1, we show that if \mathcal{F}_q contains all bounded continuous functions, then the optimal test function in PSD is

$$f_r^*(\mathbf{x}) \propto (s_p^r(\mathbf{x}) - s_q^r(\mathbf{x})) . \quad (8)$$

It can also be shown that PSD is equivalent to the *Fisher divergence*, which has been extensively used in training energy based models (Song et al., 2020; Song & Ermon, 2019) and fitting kernel exponential families (Sriperumbudur et al., 2017; Sutherland et al., 2018; Wenliang et al., 2019).

We now prove that PSD upper-bounds S_{g_r} , with the gap as the expected square error between their optimal test functions f_r^* and h_{r,g_r}^* (Proposition 3 in appendix E.2). Since PSD is constant w.r.t. \mathbf{g}_r , maximization of S_{g_r} is equivalent to a minimization task, called *controlled approximation*.

Theorem 3 (Controlled Approximation). *Assume assumptions 1-4, and the coefficient for the optimal test functions to be 1 w.l.o.g., then $\text{PSD} \geq S_{g_r}$ and*

$$\text{PSD} - S_{g_r} = \sum_{\mathbf{r} \in O_r} \mathbb{E}_q[(f_r^*(\mathbf{x}) - h_{r,g_r}^*(\mathbf{x}^T \mathbf{g}_r))^2], \quad (9)$$

with f_r^* and h_{r,g_r}^* are optimal test functions for PSD and S_{g_r} defined in Eq.8 and proposition 3 respectively.

Intuitively, minimizing the above gap can be regarded as a function approximation problem, where we want to approximate a multivariate function $f_r^* : \mathbb{R}^D \rightarrow \mathbb{R}$ by a univariate function $h_{r,g_r}^* : \mathbb{R} \rightarrow \mathbb{R}$ with optimal parameters \mathbf{g}_r .

4.2. Upper-bounding the error

Solving the controlled approximation task directly may be difficult in practice. Instead, we propose an upper-bound of the approximation error, such that this upper-bound's minimizer \mathbf{g}_r is analytic. The inspiration comes from the *active subspace method* for dimensionality reduction (Constantine et al., 2014; Zahm et al., 2020), therefore we name the corresponding minimizers as *active slices*.

Theorem 4 (Error upper-bound and active slices \mathbf{g}_r). *Assume assumptions 2 and 4-6, we can upper bound the inner part of the controlled approximation error (Eq.9) by*

$$\mathbb{E}_q \left[(f_r^*(\mathbf{x}) - h_{r,g_r}^*(\mathbf{x}^T \mathbf{g}_r))^2 \right] \leq C_{sup} \text{tr} \left(\mathbf{G}_{r \setminus d} \mathbf{H}_r \mathbf{G}_{r \setminus d}^T \right), \quad (10)$$

$$\mathbf{H}_r = \int q(\mathbf{x}) \nabla_{\mathbf{x}} f_r^*(\mathbf{x}) \nabla_{\mathbf{x}} f_r^*(\mathbf{x})^T d\mathbf{x}. \quad (11)$$

Here C_{sup} is the Poincaré constant defined in assumption 6 and $\mathbf{G}_{r \setminus d} \in \mathbb{R}^{(D-1) \times D}$ is an arbitrary orthogonal matrix \mathbf{G}_r excluding the d^{th} row \mathbf{g}_r . The orthogonal matrix has the form $\mathbf{G}_r = [\mathbf{a}_1, \dots, \mathbf{a}_D]^T$ where $\mathbf{a}_i \in \mathbb{S}^{D-1}$ and $\mathbf{a}_d = \mathbf{g}_r$.

The above upper-bound is minimized when the row space of $\mathbf{G}_{r \setminus d}$ is the span of the first $D - 1$ eigenvectors of \mathbf{H}_r

(arranging eigenvalues in ascending order). One possible choice for active slice \mathbf{g}_r is \mathbf{v}_D , where $(\lambda_i, \mathbf{v}_i)$ is the eigenpair of \mathbf{H}_r and $\lambda_1 \leq \lambda_2 \leq \dots \leq \lambda_D$.

Intuitively, the active slices $\mathbf{g}_r = \mathbf{v}_D$ are the directions where the test function f_r^* varies the most. Indeed, we have $\mathbf{v}_D^T \mathbf{H}_r \mathbf{v}_D = \mathbb{E}_q[|\nabla_{\mathbf{x}} f_r^*(\mathbf{x})^T \mathbf{v}_D|^2] = \lambda_D$, where the eigenvalue λ_D measures the averaged gradient variation in the direction defined by \mathbf{v}_D .

5. Active slice direction \mathbf{r}

The dependence of active slice \mathbf{g}_r on \mathbf{r} motivate us to consider the possible choices of \mathbf{r} . Although finite random slices \mathbf{r} are sufficient for obtaining a valid discrepancy, in practice using sub-optimal \mathbf{r} can result in weak discriminative power and poor active slices \mathbf{g}_r . We address this issue by proposing an efficient algorithm to search for good \mathbf{r} . Again all the proofs can be found in appendix G.

5.1. PSD Maximization for searching \mathbf{r}

Directly optimizing S_{r,g_r} w.r.t. \mathbf{r} is particularly difficult due to the alternated updates of \mathbf{r} and \mathbf{g}_r . To simplify the analysis, we start from the task of finding a single direction \mathbf{r} . Our key idea to sidestep such alternation is based on the intuition that S_{r,g_r} with active slices \mathbf{g}_r should well approximate PSD_r (PSD with given \mathbf{r}) from theorem 4. The independence of PSD_r to \mathbf{g}_r allows us to avoid the alternated update and the accurate approximation validates the direct usage of the resulting active slices in S_{r,g_r} . Indeed, we will prove that maximizing PSD_r is equivalent to maximizing a lower-bound for S_{r,g_r} .

Assume we have two slices \mathbf{r}_1 and \mathbf{r}_2 , with given $\mathbf{g}_{r_1}, \mathbf{g}_{r_2}$. Then finding good \mathbf{r}_1 is equivalent to maximizing the difference $S_{r_1, g_{r_1}} - S_{r_2, g_{r_2}}$. The following proposition establishes a lower-bound for this difference.

Proposition 1 (Lower-bound for the S_{r,g_r} gap). *Assume the conditions in theorem 4 are satisfied, then for any slices $\mathbf{r}_1, \mathbf{r}_2$ and $\mathbf{g}_{r_1}, \mathbf{g}_{r_2}$, we have*

$$S_{r_1, g_{r_1}} - S_{r_2, g_{r_2}} \geq \text{PSD}_{r_1} - \text{PSD}_{r_2} - C_{sup} \Omega, \quad (12)$$

where C_{sup} is the Poincaré constant defined in assumption 6 and $\Omega = \sum_{i=1}^D \omega_i$ where $\{\omega_i\}_i^D$ is the eigenvalue of $\mathbb{E}_q[\nabla_{\mathbf{x}} \mathbf{f}^*(\mathbf{x}) \nabla_{\mathbf{x}} \mathbf{f}^*(\mathbf{x})^T]$, $\mathbf{f}^*(\mathbf{x}) = s_p(\mathbf{x}) - s_q(\mathbf{x})$.

Proposition 1 justifies the maximization of PSD_{r_1} w.r.t. \mathbf{r}_1 as a valid surrogate. But more importantly, this alternative objective admits an analytic maximizer of \mathbf{r} , which is then used as the active slice direction:

Theorem 5 (Active slice \mathbf{r}). *Assuming assumptions 1-4, then the maximum of the PSD_r is achieved at $\mathbf{r}^* = \mathbf{v}_{max}$:*

$$\max_{\mathbf{r} \in \mathbb{S}^{D-1}} \mathbb{E}_q [s_p^r(\mathbf{x}) f_r^*(\mathbf{x}) + \mathbf{r}^T \nabla_{\mathbf{x}} f_r^*(\mathbf{x})] = \lambda_{max}.$$

Algorithm 1 Active slice algorithm

Input: Samples $\mathbf{x} \sim q$, density p , kernel $k : \mathcal{X} \times \mathcal{X} \rightarrow \mathbb{R}$, Gaussian noise γ , pruning factor m (optional)
Result: $\widetilde{O}_r, \mathbf{G}$
Estimate $s_p(\mathbf{x}) - s_q(\mathbf{x})$ using KE or GE with kernel k and samples \mathbf{x} .
if Pruning **then**
 Top m eigenvectors of \mathbf{S} to form \widetilde{O}_r (Theorem 5)
else
 Getting all eigenvectors of \mathbf{S} to form \widetilde{O}_r
end if
Add noise γ to \widetilde{O}_r , then normalize. (Section 3.1)
for $r \in \widetilde{O}_r$ **do**
 \mathbf{g}_r is the top 1 eigenvector of \mathbf{H}_r (Theorem 4)
 Add noise γ to \mathbf{g}_r then normalize (Section 3.1)
 Concatenate \mathbf{g}_r to \mathbf{G}
end for
Further optimize $\widetilde{O}_r, \mathbf{G}$ with $SKSD-g$ (SK_{g_r}) using gradient-based optimization (Optional)
Return: $\widetilde{O}_r, \mathbf{G}$

Here $(\lambda_{max}, \mathbf{v}_{max})$ is the largest eigenpair of the matrix $\mathbf{S} = \mathbb{E}_q [\mathbf{f}^*(\mathbf{x})\mathbf{f}^*(\mathbf{x})^T]$

5.2. Constructing the orthogonal basis O_r

Under certain scenarios, e.g. model learning, we want to train the model to perform well in every directions instead of a particular one. Thus, using a good orthogonal basis is preferred over a single active slice r . Here gradient-based optimization is less suited as it breaks the orthogonality constraint. Also proposition 1 is less useful here as well, as PSD is invariant to the choice of O_r , i.e. $\text{PSD}(q, p; O_{r_1}) = \text{PSD}(q, p; O_{r_2})$ and $O_{r_1} \neq O_{r_2}$.

Inspired by the analysis of single active r , we propose to use the eigendecomposition of \mathbf{S} to obtain a good orthogonal basis O_r . Theoretically, this operation also corresponds to a greedy algorithm, where in step i it searches for the optimal direction \mathbf{r}_i that is orthogonal to $\{\mathbf{r}_{<i}\}$ and maximizes $\text{PSD}_{\mathbf{r}_i}$ (see Corollary 6.2 in appendix G.3). Although there is no guarantee for finding the *optimal* O_r due to its myopic behavior, in practice this greedy algorithm at least finds some good directions with high discriminative power (eigenvectors with large eigenvalues).

6. Practical algorithm

The proposed active slice method is summarized in Algorithm 1, which requires the intractable score difference $s_p(\mathbf{x}) - s_q(\mathbf{x})$. Two types of approximations can be used. The first approach applies *gradient estimators* (GE) to estimate $s_q(\mathbf{x})$ from \mathbf{x} samples. We use the Stein gradient estimator

(Li & Turner, 2017) for the GE approach, although other estimators (Sriperumbudur et al., 2017; Sutherland et al., 2018; Shi et al., 2018; Zhou et al., 2020) can also be employed. The second method directly estimates the score difference using a *kernel-smoothed estimator* (KE):

$$\begin{aligned} s_p(\mathbf{y}) - s_q(\mathbf{y}) &\approx \mathbb{E}_{\mathbf{x} \sim q} [(s_p(\mathbf{x}) - s_q(\mathbf{x}))k(\mathbf{x}, \mathbf{y})] \\ &= \mathbb{E}_{\mathbf{x} \sim q} [s_p(\mathbf{x})k(\mathbf{x}, \mathbf{y}) + \nabla_{\mathbf{x}}k(\mathbf{x}, \mathbf{y})], \end{aligned} \quad (13)$$

where the second expression comes from integration by part, and it can be computed in practice. Figure 1 summarizes the relationships between different SSD discrepancies and highlights our contributions. For GOF test specifically, we also derive the asymptotic distribution and propose an practical GOF algorithm in appendix D.

7. Experiments

7.1. Benchmark GOF tests

We demonstrate the improved test power results (in terms of null rejection rates) and significant speed-ups of the proposed active slice algorithm on 3 benchmark tasks, which have been extensively used for measuring GOF test performances (Jitkrittum et al., 2017; Huggins & Mackey, 2018; Chwialkowski et al., 2016; Gong et al., 2021). Here the test statistic is based on $SKSD-g$ (SK_{g_r}) with fixed basis $O_r = \mathbf{I}$. Two practical approaches are considered for computing the active slice \mathbf{g}_r : (i) gradient estimation with the Stein gradient estimator ($SKSD-g+GE$), and (ii) gradient estimation with the kernel-smoothed estimator (KE), plus further gradient-based optimization ($SKSD-g+KE+GO$). For reference, we include a version of the algorithm with exact score difference ($SKSD-g+Ex$) as an ablation for the gradient estimation approaches.

In comparison, we include the following strong baselines: KSD with RBF kernel (Liu et al., 2016; Chwialkowski et al., 2016), maximum mean discrepancy (MMD, Gretton et al., 2012) with RBF kernel, random feature Stein discrepancy with L1 IMQ kernel (L1-IMQ, Huggins & Mackey, 2018), and the current state-of-the-art — $maxSKSD-g$ with random initialized \mathbf{g}_r followed by gradient optimization ($SKSD-g+GO$, Gong et al., 2021). For all methods requiring GO or active slices, we split the 1000 test samples from q into 800 test and 200 training data, where we run GO or active slice method on the training set.

The 3 GOF test benchmarks, with details in appendix H.1, are: (1) **Laplace:** $p(\mathbf{x}) = \mathcal{N}(0, \mathbf{I})$, $q(\mathbf{x}) = \prod_{d=1}^D \text{Lap}(x_d | 0, 1/\sqrt{2})$; (2) **Multivariate-t:** $p(\mathbf{x}) = \mathcal{N}(0, \frac{5}{3}\mathbf{I})$, $q(\mathbf{x})$ is a fully factorized multivariate-t with 5 degrees of freedom, 0 mean and scale 1; (3) **Diffusion:** $p(\mathbf{x}) = \mathcal{N}(0, \mathbf{I})$, $q(\mathbf{x}) = \mathcal{N}(\mathbf{0}, \Sigma_1)$ where in $q(\mathbf{x})$ the variance of 1st-dim is 0.3 and the rest is \mathbf{I} .

The upper panels in Figure 2 show the test power re-

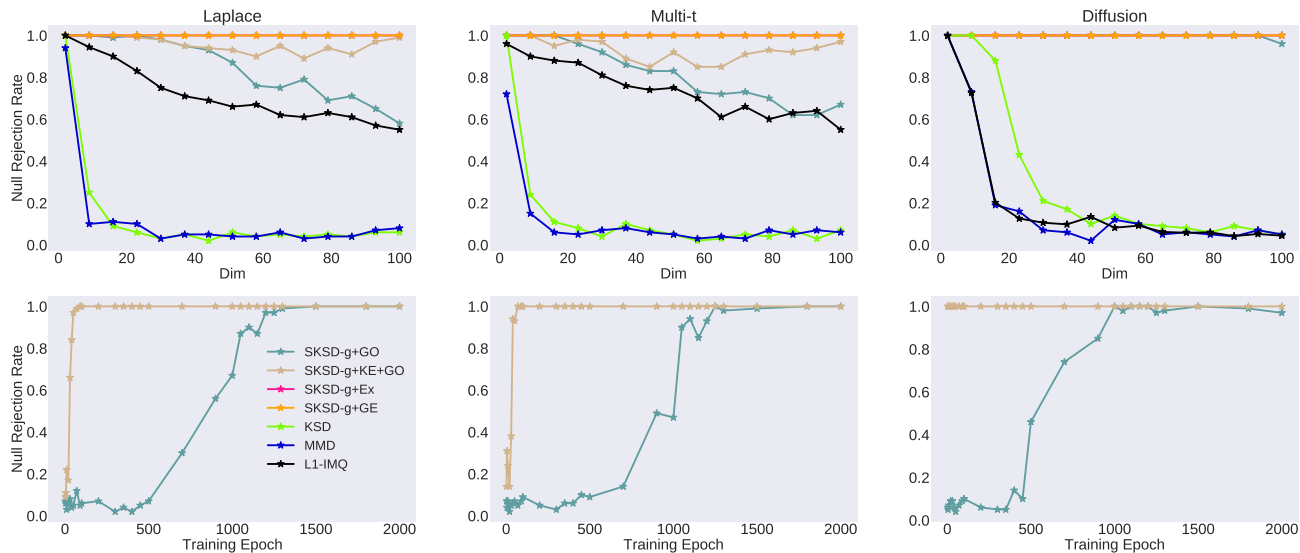


Figure 2. (**Upper panel**): The null rejection rate w.r.t. different dimensional benchmark problems. *SKSD-g+Ex* and *SKSD-g+GE* coincide at the optimal rejection rate (**Lower panel**): Null rejection rate with different number of gradient optimization epochs.

sults as the dimensions D increase. As expected, *KSD* and *MMD* with RBF kernel suffer from the curse-of-dimensionality. *L1-IMQ* performs relatively well in **Laplace** and **multivariate-t** but still fails in **diffusion**. For SKSD based approaches, *SKSD-g+GO* with 1000 training epochs still exhibits a decreasing test power in **Laplace** and **multivariate-t**. On the other hand, *SKSD-g+KE+GO* with 50 training epochs has nearly optimal performance. *SKSD-g+Ex* and *SKSD-g+GE* achieve the true optimal rejection rate without any *GO*. Specifically, Table 1 shows that the active slice method achieves significant computational savings with **14x-80x** speed-up over *SKSD-g+GO*.

For approaches that require gradient optimization, the lower panels in Figure 2 show the test power as the number of training epochs increases. *SKSD-g+GO* with random slice initialization requires a huge number of gradient updates to obtain reasonable test power, and 1000 epochs achieves the best balance between run-time and performance. On the other hand, *SKSD-g+KE+GO* with active slice achieves significant speed-ups with near-optimal test power using around **50** epochs on **Laplace** and **Multivariate-t**. Remarkably, on **Diffusion** test, g_r initialized by the active slices achieves near-optimal results already, so that the later gradient refinements are not required.

7.2. RBM GOF test

Following Gong et al. (2021), we conduct a more complex GOF test using restrict Boltzman machines (RBMs, (Hinton & Salakhutdinov, 2006; Welling et al.)). Here the p distribution is an RBM: $p(\mathbf{x}) =$

$\frac{1}{Z} \exp(\mathbf{x}^\top \mathbf{B} \mathbf{h} + \mathbf{b}^\top \mathbf{x} + \mathbf{c}^\top \mathbf{x} - \frac{1}{2} \|\mathbf{x}\|^2)$, where $\mathbf{x} \in \mathbb{R}^D$ and $\mathbf{h} \in \{\pm 1\}^{d_h}$ denotes the hidden variables. The q distribution is also an RBM with the same \mathbf{b}, \mathbf{c} parameters as p but a different \mathbf{B} matrix perturbed by different levels of Gaussian noise. We use $D = 50$ and $d_h = 40$, and block Gibbs sampler with 2000 burn-in steps. The test statistics for all the approaches are computed on a test set containing 1000 samples from q .

The test statistic is constructed using *SKSD-rg* (SK_{rg_r}) with r, g_r obtained either by gradient-based optimization (*SKSD-rg+GO*) or the active slice algorithms (+*KE*, +*GE* and +*Ex*) without the gradient refinements. Specifically, *SKSD-rg+GO* runs 50 training epochs with r and g_r initialized to \mathbf{I} . For the active slice methods, we also prune away most slices and only keep the top-3 most important r slices.

The left panel of Figure 3 shows that *SKSD-rg+KE* achieves the best null rejection rates among all baselines, except for *SKSD-rg+Ex* whose performance is expected to upper-bound all other active slice methods. This shows the potential of our approach with an accurate score difference estimator. Although *SKSD-rg+GO* performs reasonably well, its run-time is **53x** longer than *SKSD-rg+KE* as shown in Table 3. Interestingly, *SKSD-rg+GE* performs worse than *KSD* due to the significant under-estimation of the magnitude of $s_q(\mathbf{x})$. Therefore, we omit this approach in the following ablation studies.

Ablation studies The first ablation study, with results shown in the middle panel in Figure 3, considers pruning the active slices at different pruning levels, where the horizontal

Table 1. Test power for 100 dimensional benchmarks and time consumption. The run-time for SKSD-g+KE+GO include both the active slice computation and the later gradient-based refinement steps. NRR stands for null rejection rate.

Method	Laplace			Multi-t			Diffusion		
	NRR	sec/trial	Speed-up	NRR	sec/trial	Speed-up	NRR	sec/trial	Speed-up
SKSD-g+Ex	1	0.38	103x	1	0.49	90x	1	0.34	102x
SKSD-g+GO	0.58	39.39	1x	0.67	44.24	1x	0.96	34.73	1x
SKSD-g+KE+GO	0.99	2.72	14x	0.97	2.38	19x	1	0.43	81x
SKSD-g+GE	1	0.66	60x	1	0.67	66x	1	0.78	44x

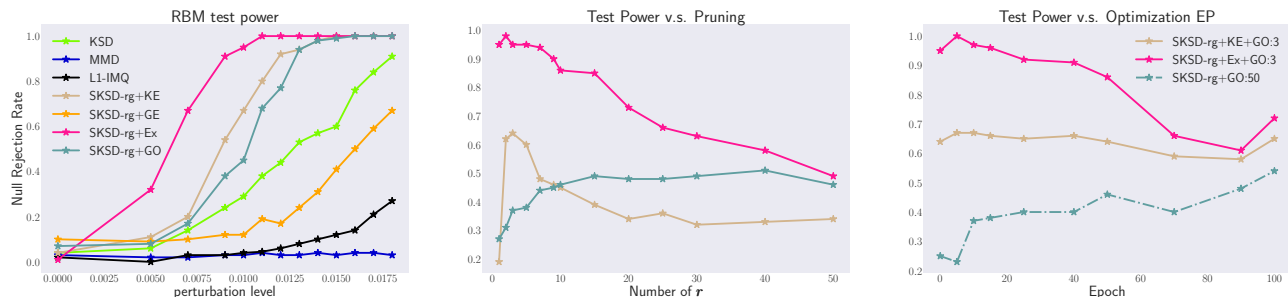


Figure 3. (Left): The GOF test power of each method with different level of noise perturbations (Mid): The effect of different pruning level towards the test power (Right): The effect of gradient based optimization epoch to the test power. 3 and 50 indicates the pruning level. *KE+GO* or *Ex+GO* means active slices with further gradient refinement steps.

axis indicates the number of r slices used to construct the test statistic. We observe that the null rejection rates of active slice methods peak with pruning level 3, indicating their ability to select the most important directions. Their performances decrease when more r are considered since, in practice, those less important directions introduce extra noise to the test statistic. On the other hand, *SKSD-rg+GO* shows no pruning abilities due to its sensitivity to slice initialization. Remarkably, the final performance of *SKSD-rg+GO* without pruning is still worse than *SKSD-rg+KE* with pruning, showing the importance of finding 'good' instead of many 'average-quality' directions. Another advantage of pruning is to reduce the computational and memory costs from $O(MD)$ to $O(mD)$, where m and M are the number of pruned r and slice initializations, respectively ($m \ll M$).

The second ablation study investigates the quality of the obtained slices either by gradient-based optimization or by the active slice approaches. Results are shown in the right panel of Figure 3, where the horizontal axis indicates the number of training epochs, and the numbers annotated in the legend (3 and 50) indicate the pruning. We observe that the null rejection rate of *SKSD-rg+KE+GO* starts to improve only after 100 epochs, meaning that short run of *GO* refinements are redundant due to the good quality of active slices. The performance decrease of *SKSD-rg+Ex+GO* is due to the over-fitting of *GO* to the training set. The null rejection rate of *SKSD-rg+GO* gradually increases with larger training epochs as expected. However, even after 100 epochs, the test power is still lower than active slices without any *GO*.

In appendix H.2, another ablation study also shows the advantages of good r compared to using random slices.

7.3. Model learning: ICA

We evaluate the performance of the active slice methods in model learning by training an independent component analysis (ICA) model, which has been extensively used to evaluate algorithms for training energy-based models (Gutmann & Hyvärinen, 2010; Hyvärinen & Dayan, 2005; Ceylan & Gutmann, 2018; Grathwohl et al., 2020). ICA follows a simple generative process: it first samples a D -dimensional random variable z from a non-Gaussian p_z (we use multivariate-t), then transforms z to $x = Wz$ with a non-singular matrix $W \in \mathbb{R}^{D \times D}$. The log-likelihood is $\log p(x) = \log p_z(W^{-1}x) + C$ where C can be ignored if trained by minimizing Stein discrepancies. We follow Grathwohl et al. (2020); Gong et al. (2021) to sample 20000 training and 5000 test datapoints from a randomly initialized ICA model. The baselines considered include *KSD*, *SKSD-g+GO*, *SKSD-rg+GO* and the state-of-the-art *learned Stein discrepancy (LSD)* (Grathwohl et al., 2020), where the test function is parametrized by a neural network. For active slice approaches, one optimization epoch include the following two steps: (i) finding active slices for both orthogonal basis O_r and g_r at the beginning of the epoch, and (ii) refining the g_r directions and the W parameters in an adversarial manner with O_r fixed. For *SKSD-g+GO*, we fix basis $O_r = I$ and only update g_r with *GO*. We refer to appendix H.3 for details on the setup and training procedure. We see

Table 2. The test NLL of different dimensional ICA model

Dimensions	SKSD-g+KE+GO	SKSD-g+Ex+GO	SKSD-g+GO	SKSD-rg+GO	LSD	KSD
10	7.93±0.31	7.95±0.31	8.06±0.33	10.03±0.61	7.42±0.31	7.82±0.31
80	7.88±0.77	15.17±0.97	19.03±1.06	62.53±0.92	6.26±1.49	80.75±1.22
100	6.93±1.36	21.50±1.41	22.22±1.08	75.28±1.63	17.55±1.60	110.78±1.19
150	11.67±2.46	27.37±3.04	21.63±3.27	107.25±1.93	32.15±3.75	180.47±1.91

Table 3. Test power and time consumption at 0.01 perturbation

	Test Power	Opt. Time	Speed-up
SKSD-rg+Ex	0.95	0.04s	254x
SKSD-rg+KE	0.67	0.19s	53x
SKSD-rg+GO	0.45	10.15s	1x



Figure 4. Training Curve of ICA model, where y-axis indicates the test NLL.

from Figure 4 that *SKSD-g+KE+GO* converges significantly faster at 150 dimensions than all baselines; moreover, it has much better NLL (Table 2). We argue this performance gain is due to the use of the better orthogonal basis O_r found by the greedy algorithm, showing the advantages of better O_r in model learning. On the other hand, the importance of orthogonality in O_r is indicated by the poor performance of *SKSD-rg+GO*, as gradient updates for r violate the orthogonality constraint. The goal of learning is to train the model to match the data distribution along every slicing direction, and the orthogonality constraint can help prevent the model from ignoring important slicing directions.

Interestingly, *SKSD-g+Ex+GO* performs worse than *+KE+GO*. We hypothesize that this is because the *+Ex+GO* approach often focuses on directions with large discriminative power but with less useful learning signal (see appendix H.3). *LSD* performs well in low dimensional problems. However, in high dimensional learning tasks it spends too much time on finding good test functions, which slows down the convergence significantly.

8. Related Work

Active subspace method (ASM): ASM is initially proposed as a dimensionality reduction method, which constructs a subspace with low-rank projectors (Constantine et al., 2014) according to the subspace Poincaré inequality. Zahm et al. (2020) showed promising results on the application of ASM to approximating multivariate functions with lower dimensional ones. However, they only considered the subspace Poincaré inequality under Gaussian measures, and a generalization to a broader family of family is proposed by Parente et al. (2020). Another closely related approach uses logarithmic Sobolev inequality instead to construct the active subspace (Zahm et al., 2018), which can be interpreted as finding the optimal subspace to minimize a KL-divergence. It has shown successes in Bayesian inverse problems and particle inference (Chen et al., 2019).

Sliced discrepancies: Existing examples of sliced discrepancies can be roughly divided into two groups. Most of them belong to the first group, and they use the slicing idea to improve computational efficiency. For example, sliced Wasserstein distance projects distributions onto one dimensional slices so that the corresponding distance has an analytic form (Kolouri et al., 2019; Deshpande et al., 2019). Sliced score matching uses Hutchinson’s trick to avoid the expensive computation of the Hessian matrix (Song et al., 2020). The second group focuses on the curse-of-dimensionality issue which remains to be addressed. To the best of our knowledge, existing integral probability metrics in this category include *SSD* (Gong et al., 2021) and *kernelized complete conditional Stein discrepancy* (KCC-SD, Singhal et al., 2019). The former is more general and requires less restrictive assumptions, while the latter requires samples from complete conditional distributions. Recent work has also investigated the statistical properties of sliced discrepancies (Nadjahi et al., 2020).

9. Conclusion

We have proposed the active slice method as a practical solution for searching good slicing directions for *SKSD*. We first prove that the validity of the kernelized discrepancy only requires finite number of random slices instead of optimal ones, giving us huge freedom to select slice directions. Then by analyzing the approximation quality of *SSD* to *SKSD*, we

proposed to find active slices by optimizing surrogate optimization tasks. Experiments on high-dimensional GOF tests and ICA training showed the active slice method performed the best across a number of competitive baselines in terms of both test performance and run-time. Future research directions include better score difference estimation methods, non-linear generalizations of slice projections, and the application of the active slice method to other discrepancies such as MMD (Gretton et al., 2012) and sliced Wasserstein distances (Deshpande et al., 2019; Kolouri et al., 2019).

References

- Arcones, M. A. and Gine, E. On the bootstrap of u and v statistics. *The Annals of Statistics*, pp. 655–674, 1992.
- Ceylan, C. and Gutmann, M. U. Conditional noise-contrastive estimation of unnormalised models. In *International Conference on Machine Learning*, pp. 726–734. PMLR, 2018.
- Chen, P., Wu, K., Chen, J., O’Leary-Roseberry, T., and Ghattas, O. Projected stein variational newton: A fast and scalable bayesian inference method in high dimensions. *arXiv preprint arXiv:1901.08659*, 2019.
- Chwialkowski, K., Strathmann, H., and Gretton, A. A kernel test of goodness of fit. *JMLR: Workshop and Conference Proceedings*, 2016.
- Comon, P. Independent component analysis, a new concept? *Signal processing*, 36(3):287–314, 1994.
- Constantine, P. G., Dow, E., and Wang, Q. Active subspace methods in theory and practice: applications to kriging surfaces. *SIAM Journal on Scientific Computing*, 36(4): A1500–A1524, 2014.
- Deshpande, I., Hu, Y.-T., Sun, R., Pyrros, A., Siddiqui, N., Koyejo, S., Zhao, Z., Forsyth, D., and Schwing, A. G. Max-sliced wasserstein distance and its use for gans. In *Proceedings of the IEEE/CVF Conference on Computer Vision and Pattern Recognition*, pp. 10648–10656, 2019.
- Gong, W., Li, Y., and Hernández-Lobato, J. M. Sliced kernelized stein discrepancy. In *International Conference on Learning Representations*, 2021. URL <https://openreview.net/forum?id=t0TaKv0Gx6Z>.
- Gorham, J. and Mackey, L. Measuring sample quality with stein’s method. In *Advances in Neural Information Processing Systems*, pp. 226–234, 2015.
- Gorham, J. and Mackey, L. Measuring sample quality with kernels. In *International Conference on Machine Learning*, pp. 1292–1301. PMLR, 2017.
- Grathwohl, W., Wang, K.-C., Jacobsen, J.-H., Duvenaud, D., and Zemel, R. Cutting out the middle-man: Training and evaluating energy-based models without sampling. *arXiv preprint arXiv:2002.05616*, 2020.
- Gretton, A., Borgwardt, K. M., Rasch, M. J., Schölkopf, B., and Smola, A. A kernel two-sample test. *The Journal of Machine Learning Research*, 13(1):723–773, 2012.
- Gutmann, M. and Hyvärinen, A. Noise-contrastive estimation: A new estimation principle for unnormalized statistical models. In *Proceedings of the Thirteenth International Conference on Artificial Intelligence and Statistics*, pp. 297–304. *JMLR Workshop and Conference Proceedings*, 2010.
- Hinton, G. E. and Salakhutdinov, R. R. Reducing the dimensionality of data with neural networks. *science*, 313(5786):504–507, 2006.
- Hoeffding, W. A class of statistics with asymptotically normal distribution. In *Breakthroughs in statistics*, pp. 308–334. Springer, 1992.
- Hu, T., Chen, Z., Sun, H., Bai, J., Ye, M., and Cheng, G. Stein neural sampler. *arXiv preprint arXiv:1810.03545*, 2018.
- Huggins, J. and Mackey, L. Random feature stein discrepancies. In *Advances in Neural Information Processing Systems*, pp. 1899–1909, 2018.
- Huskova, M. and Janssen, P. Consistency of the generalized bootstrap for degenerate u -statistics. *The Annals of Statistics*, pp. 1811–1823, 1993.
- Hyvärinen, A. and Dayan, P. Estimation of non-normalized statistical models by score matching. *Journal of Machine Learning Research*, 6(4), 2005.
- Jitkrittum, W., Xu, W., Szabó, Z., Fukumizu, K., and Gretton, A. A linear-time kernel goodness-of-fit test. In *Advances in Neural Information Processing Systems*, pp. 262–271, 2017.
- Kingma, D. P. and Ba, J. Adam: A method for stochastic optimization. *arXiv preprint arXiv:1412.6980*, 2014.
- Kolouri, S., Nadjahi, K., Simsekli, U., Badeau, R., and Rohde, G. K. Generalized sliced wasserstein distances. *arXiv preprint arXiv:1902.00434*, 2019.
- Li, Y. and Turner, R. E. Gradient estimators for implicit models. *arXiv preprint arXiv:1705.07107*, 2017.
- Liu, Q. and Wang, D. Stein variational gradient descent: A general purpose bayesian inference algorithm. *arXiv preprint arXiv:1608.04471*, 2016.
- Liu, Q., Lee, J., and Jordan, M. A kernelized stein discrepancy for goodness-of-fit tests. In *International conference on machine learning*, pp. 276–284, 2016.
- Mityagin, B. The zero set of a real analytic function. *arXiv preprint arXiv:1512.07276*, 2015.
- Nadjahi, K., Durmus, A., Chizat, L., Kolouri, S., Shahrampour, S., and Şimşekli, U. Statistical and topological properties of sliced probability divergences. *arXiv preprint arXiv:2003.05783*, 2020.

- Parente, M. T., Wallin, J., Wohlmuth, B., et al. Generalized bounds for active subspaces. *Electronic Journal of Statistics*, 14(1):917–943, 2020.
- Pu, Y., Gan, Z., Henao, R., Li, C., Han, S., and Carin, L. Vae learning via stein variational gradient descent. *arXiv preprint arXiv:1704.05155*, 2017.
- Sameh, A. and Tong, Z. The trace minimization method for the symmetric generalized eigenvalue problem. *Journal of computational and applied mathematics*, 123(1-2):155–175, 2000.
- Serfling, R. J. *Approximation theorems of mathematical statistics*, volume 162. John Wiley & Sons, 2009.
- Shi, J., Sun, S., and Zhu, J. A spectral approach to gradient estimation for implicit distributions. *arXiv preprint arXiv:1806.02925*, 2018.
- Singhal, R., Han, X., Lahlou, S., and Ranganath, R. Kernelized complete conditional stein discrepancy. *arXiv preprint arXiv:1904.04478*, 2019.
- Song, Y. and Ermon, S. Generative modeling by estimating gradients of the data distribution. In *Advances in Neural Information Processing Systems*, pp. 11918–11930, 2019.
- Song, Y., Garg, S., Shi, J., and Ermon, S. Sliced score matching: A scalable approach to density and score estimation. In *Uncertainty in Artificial Intelligence*, pp. 574–584. PMLR, 2020.
- Sriperumbudur, B., Fukumizu, K., Gretton, A., Hyvärinen, A., and Kumar, R. Density estimation in infinite dimensional exponential families. *The Journal of Machine Learning Research*, 18(1):1830–1888, 2017.
- Sriperumbudur, B. K., Fukumizu, K., and Lanckriet, G. R. Universality, characteristic kernels and rkhs embedding of measures. *Journal of Machine Learning Research*, 12(7), 2011.
- Sutherland, D., Strathmann, H., Arbel, M., and Gretton, A. Efficient and principled score estimation with nyström kernel exponential families. In *International Conference on Artificial Intelligence and Statistics*, pp. 652–660. PMLR, 2018.
- Welling, M., Rosen-Zvi, M., and Hinton, G. E. Exponential family harmoniums with an application to information retrieval. Citeseer.
- Wenliang, L., Sutherland, D., Strathmann, H., and Gretton, A. Learning deep kernels for exponential family densities. In *International Conference on Machine Learning*, pp. 6737–6746. PMLR, 2019.
- Zahm, O., Cui, T., Law, K., Spantini, A., and Marzouk, Y. Certified dimension reduction in nonlinear bayesian inverse problems. *arXiv preprint arXiv:1807.03712*, 2018.
- Zahm, O., Constantine, P. G., Prieur, C., and Marzouk, Y. M. Gradient-based dimension reduction of multivariate vector-valued functions. *SIAM Journal on Scientific Computing*, 42(1):A534–A558, 2020.
- Zhou, Y., Shi, J., and Zhu, J. Nonparametric score estimators. *arXiv preprint arXiv:2005.10099*, 2020.

A. Terms and Notations

For the clarity of the paper, we give a summary of the commonly used notations in the main text and proof.

Symbols:

$\mathbf{s}_p(\mathbf{x})$	$\nabla_{\mathbf{x}} \log p(\mathbf{x})$
$\mathbf{s}_p^r(\mathbf{x})$	Projected score function $\nabla_{\mathbf{x}} \log p(\mathbf{x})^T \mathbf{r}$
\mathcal{X}	A subset of \mathbb{R}^D
\mathcal{K}	A subset of \mathbb{R} .
k_{r, g_r}	kernel function $k : \mathcal{K} \times \mathcal{K} \rightarrow \mathcal{R}$
\mathcal{H}_{r, g_r}	Induced RKHS by the kernel k_{r, g_r} .
$\ \cdot\ _{\mathcal{H}_{r, g_r}}$	RKHS norm of \mathcal{H}_{r, g_r}
\mathbf{g}_r	Input projection direction (e.g. $\mathbf{x}^T \mathbf{g}_r$) for corresponding \mathbf{r} .
\mathbf{r}	Score projection direction (e.g. $\mathbf{s}_p^r(\mathbf{x}) = \mathbf{s}_p(\mathbf{x})^T \mathbf{r}$)
$S_{\max_{g_r}}$	maxSSD-g (Eq.4).
S_{g_r}	SSD-g, i.e. $S_{\max_{g_r}}$ (Eq.4) without \sup_{g_r} . But with summation of O_r .
S_{r, g_r}	SSD-r, i.e. $S_{\max_{g_r}}$ (Eq.4) without \sup_{g_r} and summation of O_r . Instead, we use specific \mathbf{r} .
$SK_{\max_{g_r}}$	maxSKSD-g. The kernelized version of $S_{\max_{g_r}}$
SK_{g_r}	SKSD-g. The kernelized version of S_{g_r}
SK_{r, g_r}	SKSD-r, i.e. S_{r, g_r}
PSD	Projected Stein discrepancy (Eq.7)
PSD $_r$	Projected Stein discrepancy (Eq.7) without summation O_r and use specific \mathbf{r} instead.
f_r^*	Optimal test function for PSD. $f_r^*(\mathbf{x}) \propto \mathbf{s}_p^r(\mathbf{x}) - \mathbf{s}_q^r(\mathbf{x})$
h_{r, g_r}^*	Optimal test function for S_{g_r} with specific \mathbf{r} and \mathbf{g}_r , defined in Eq.37.
*	This indicates the optimal test function (e.g. f_r^*)
C_{\sup}	Supremum of Poincaré constant defined in assumption 6.

B. Assumptions and Definitions

Definition B.1 (Inner product in Hilbert space). *We denote the algebraic space \mathbb{R}^D refers to a parameter space of dimension D . The Borel sets of \mathbb{R}^D is denoted as $\mathcal{B}(\mathbb{R}^D)$, and we let $\mu(x)$ be a probability measure on \mathbf{x} . We define*

$$\mathcal{H}_{\mu} = L^2(\mathbb{R}^D, \mathcal{B}(\mathbb{R}^D), \mu) \quad (14)$$

as the Hilbert space which contains all the measurable functions $f : \mathbb{R}^D \rightarrow \mathbb{R}$, such that $\|f\|_{\mathcal{H}_{\mu}} \leq \infty$, where we define inner product $\langle \cdot, \cdot \rangle_{\mathcal{H}_{\mu}}$ to be

$$\langle f, g \rangle_{\mathcal{H}_{\mu}} = \int f(\mathbf{x})g(\mathbf{x})d\mu(\mathbf{x}) \quad (15)$$

for all $f, g \in \mathcal{H}_{\mu}$

Definition B.2. (*Stein Class (Liu et al., 2016)*) *Assume distribution q has continuous and differentiable density $q(\mathbf{x})$. A function f defined on the domain $\mathcal{X} \subseteq \mathbb{R}^D$, $f : \mathcal{X} \rightarrow \mathbb{R}$ is in the **Stein class** of q if f is smooth and satisfies*

$$\int_{\mathcal{X}} \nabla_{\mathbf{x}}(f(\mathbf{x})q(\mathbf{x}))d\mathbf{x} = 0 \quad (16)$$

We call a function $f(\mathbf{x}) \in \mathcal{F}_q$ if f belongs to the Stein class of q . We say vector-valued function $\mathbf{f}(\mathbf{x}) : \mathcal{X} \subseteq \mathbb{R}^D \rightarrow \mathbb{R}^m \in \mathcal{F}_q$ if each component of \mathbf{f} belongs to the Stein class of q .

Definition B.3 (Stein Identity). *Assume q is a smooth density satisfied assumption 1, then we have*

$$\mathbb{E}_q [s_q(\mathbf{x})f(\mathbf{x})^T + \nabla f(\mathbf{x})] = 0 \quad (17)$$

for any functions $f : \mathcal{X} \subseteq \mathbb{R}^D \rightarrow \mathbb{R}^D$ in Stein class of q .

We can easily see that the above holds true for $\mathcal{X} = \mathbb{R}^D$ if

$$\lim_{\|\mathbf{x}\| \rightarrow \infty} q(\mathbf{x})f(\mathbf{x}) = 0 \quad (18)$$

Assumption 1 (Properties of densities) Assume the two probability distributions p, q has continuous differentiable density $p(\mathbf{x}), q(\mathbf{x})$ supported on $\mathcal{X} \subseteq \mathbb{R}^D$, such that the induced set $\mathcal{K} = \{y \in \mathbb{R} | y = \mathbf{x}^T \mathbf{g}, \|\mathbf{g}\|^2 = 1, \mathbf{x} \in \mathcal{X}\}$ is *locally compact Hausdorff (LCH)* for all possible $\mathbf{g} \in \mathbb{S}^{D-1}$. If $\mathcal{X} = \mathbb{R}^D$, then the density q satisfies: $\lim_{\|\mathbf{x}\| \rightarrow \infty} q(\mathbf{x}) = 0$. If $\mathcal{X} \subset \mathbb{R}^D$ is compact, then $q(\mathbf{x}) = 0$ at boundary $\partial \mathcal{X}$.

Assumption 2 (Regularity of score functions) Denote the score function of $p(\mathbf{x})$ as $\mathbf{s}_p(\mathbf{x}) = \nabla_{\mathbf{x}} \log p(\mathbf{x}) \in \mathbb{R}^D$ and score function of $q(\mathbf{x})$ accordingly. Assume the score functions are bounded continuous differentiable functions and satisfying

$$\begin{aligned} \int_{\mathcal{X}} q(\mathbf{x})|(s_p(\mathbf{x}) - s_q(\mathbf{x}))^T \mathbf{r}|d\mathbf{x} < \infty \\ \int_{\mathcal{X}} q(\mathbf{x})\|(s_p(\mathbf{x}) - s_q(\mathbf{x}))^T \mathbf{r}\|^2 d\mathbf{x} < \infty \end{aligned} \quad (19)$$

for all \mathbf{r} where $\mathbf{r} \in \mathbb{S}^{D-1}$.

Assumption 3 (Test functions) Assume the test function $h_{r, g_r} : \mathcal{K} \subseteq \mathbb{R} \rightarrow \mathbb{R}$ is smooth and belongs to the Stein class of q . Specifically, if with assumption 1, we only requires h_{r, g_r} to be a bounded continuous function. Similarly, we assume this also holds for PSD (eq.7) test function $f_r(\mathbf{x})$.

Assumption 4 (Bounded Conditional Expectation) Define

$$h_{r, g_r}^*(y_a) = \mathbb{E}_{q_{G_r}(\mathbf{y}-a|y_a)}[(s_p^r(\mathbf{G}_r^{-1}\mathbf{y}) - s_q^r(\mathbf{G}_r^{-1}\mathbf{y}))] \quad (20)$$

as in proposition 3. We assume h_{r, g_r}^* is uniformly bounded for all possible $\mathbf{g}_r \in \mathbb{S}^{D-1}$.

Assumption 5 (Log-concave probabilities) Assume a probability distribution q with density function such that $q(\mathbf{x}) = \exp(-V(\mathbf{x}))$, where $V(\mathbf{x})$ is a convex function.

Assumption 6 (Existence of supremum of Poincaré constant). For the Poincaré constant defined in lemma 5, the essential supremum exists $C_{ess, \mathbf{G}} = \text{ess sup}_{y_d} C_{y_d} < \infty$ and also the $C_{sup} = \sup_{\mathbf{G}} C_{ess, \mathbf{G}} < \infty$ exists over all possible orthogonal matrix \mathbf{G} .

Assumption 7 (universal kernel): We assume the kernel $k_{rg} : \mathcal{K} \times \mathcal{K} \rightarrow \mathbb{R}$ is bounded and c_0 -universal.

Assumption 8 (Real analytic translation invariant kernel): We assume the kernel is translation invariant $k(x, y) = \phi(x - y) : \mathcal{K} \rightarrow \mathbb{R}$ and ϕ is a real analytic function. Additionally, we assume if $k(cx, cy) = k'(x, y)$ for a constant $c > 0$ where k' is also a c_0 -universal kernel. For example, *radial basis kernel function* (RBF) and *inverse multiquadric* (IMQ) kernel satisfy these assumptions.

The assumption 1-4 are used for defining the SSD family. Assumptions 5-6 are used for subspace Poincaré inequality. Assumption 7 is used for the validity of *maxSKSD-g* and *maxSKSD-rg*. In addition, if the kernel k_{rg} is defined in the *locally compact Hausdorff* (LCH) space (e.g. \mathbb{R}), the resulting RKHS induced by k_{rg} is c_0 -universal and L_p -universal (Sriperumbudur et al., 2011). Assumption 8 is used to analyze the real analyticity of *maxSKSD-g* w.r.t. \mathbf{g}_r .

C. Detailed Background

C.1. Sliced Stein Discrepancy

In this section, we give a more detailed introduction to sliced Stein discrepancy (SSD) and its variants. Recall the definition of Stein discrepancy:

$$D_{SD}(q, p) = \sup_{\mathbf{f} \in \mathcal{F}_q} \mathbb{E}_q[\mathbf{s}_p^T(\mathbf{x})\mathbf{f}(\mathbf{x}) + \nabla_{\mathbf{x}}^T \mathbf{f}(\mathbf{x})] \quad (21)$$

In the original paper of (Gong et al., 2021), they argue that the curse of dimensionality comes from two sources: (i) the high dimensionality of the score function $\mathbf{s}_p : \mathcal{X} \subseteq \mathbb{R}^D \rightarrow \mathbb{R}^D$ and (ii) the test function input $\mathbf{x} \in \mathcal{X} \subseteq \mathbb{R}^D$. Therefore, authors proposed two slice directions \mathbf{r}, \mathbf{g} to project \mathbf{s}_p and \mathbf{x} respectively. However, this projection is equivalent to throwing away most of the information possessed by \mathbf{s}_p and \mathbf{x} , which may results in the violation of the discrepancy validity. To tackle this problem, authors proposed the first member of the SSD family by considering over all possible directions of \mathbf{r} and \mathbf{g} (a distribution over $\mathbf{r} \sim p_r, \mathbf{g} \sim p_g$),

called *integrated sliced Stein discrepancy*:

$$S(q, p) = \mathbb{E}_{p_r, p_g} \left[\sup_{h_{rg} \in \mathcal{F}_q} \mathbb{E}_q[\mathbf{s}_p^T(\mathbf{x})h_{rg}(\mathbf{x}^T \mathbf{g}) + \mathbf{r}^T \mathbf{g} \nabla_{\mathbf{x}^T \mathbf{g}} h_{rg}(\mathbf{x}^T \mathbf{g})] \right] \quad (22)$$

where h_{rg} is the test function. Although it is theoretically valid (Theorem 1 in (Gong et al., 2021)), its practical useage is limited by the intractability of the integral over p_r, p_g and the optimal test function h_{rg} . Fortunately, authors show that integral is not necessary for discrepancy validity, and can be replaced by summation over an orthogonal basis of $\mathbf{r} \in O_r$ with corresponding optimal \mathbf{g}_r . This second member of SSD family is called *maxSSD-g* defined in the main text by Eq.4 ($S_{\max_{g_r}}$). Further, one can also use single optimal direction \mathbf{r} to replace the summation over the orthogonal basis O_r , resulting in the third member called *maxSSD-rg* ($S_{\max_{rg}}$):

$$S_{\max_{rg}}(q, p) = \sup_{h_{rg} \in \mathcal{F}_q, \mathbf{g}_r, \mathbf{r} \in \mathbb{S}^{D-1}} \mathbb{E}_q[\mathbf{s}_p^T(\mathbf{x})h_{rg}(\mathbf{x}^T \mathbf{g}_r) + \mathbf{r}^T \mathbf{g}_r \nabla_{\mathbf{x}^T \mathbf{g}_r} h_{rg}(\mathbf{x}^T \mathbf{g}_r)] \quad (23)$$

It is worth noting that there is one more valid member of the SSD family, called *orthogonal sliced Stein discrepancy*, which only replace the integral of $p_r(\mathbf{r})$ with summation over O_r . Namely, it is defined as *integrated SSD* (Eq.22) where the integral of p_r is replaced by summation over orthogonal basis O_r .

$$S_O(q, p) = \sum_{\mathbf{r} \in O_r} \mathbb{E}_{p_g} \left[\sup_{h_{rg} \in \mathcal{F}_q} \mathbb{E}_q[\mathbf{s}_p^T(\mathbf{x})h_{rg}(\mathbf{x}^T \mathbf{g}) + \mathbf{r}^T \mathbf{g} \nabla_{\mathbf{x}^T \mathbf{g}} h_{rg}(\mathbf{x}^T \mathbf{g})] \right] \quad (24)$$

Authors addressed tractability issue of the optimal h_{rg} by restricting the \mathcal{F}_q to be a one-dimensional RKHS induced by a c_0 -universal kernel $k_{rg} : \mathcal{K} \times \mathcal{K} \rightarrow \mathbb{R}$ where $\mathcal{K} \subseteq \mathbb{R}$. Thus, for each member of the above SSD family, we have a corresponding kernelized version. They are called *integrated sliced kernelized Stein discrepancy*, *max sliced kernelized Stein discrepancy* (*maxSKSD* family includes *maxSKSD-g* and *maxSKSD-rg*), and *orthogonal SKSD*. In practice, *maxSKSD* is often preferred over the others due to its computational tractability, where their optimal slices for \mathbf{r} and \mathbf{g}_r are obtained by gradient-based optimization.

We already have $\xi_{p_r, g_r}(\mathbf{x}, \cdot)$ defined in Eq.5. We further

define

$$\begin{aligned} \mu_{p,r,g_r}(\mathbf{x}, \mathbf{y}) &= s_p^r(\mathbf{x})k_{rg_r}(\mathbf{x}^T \mathbf{g}_r, \mathbf{y}^T \mathbf{g}_r)s_p^r(\mathbf{y}) \\ &\quad + \mathbf{r}^T \mathbf{g}_r s_p^r(\mathbf{y}) \nabla_{\mathbf{x}^T \mathbf{g}_r} k_{rg_r}(\mathbf{x}^T \mathbf{g}_r, \mathbf{y}^T \mathbf{g}_r) \\ &\quad + \mathbf{r}^T \mathbf{g}_r s_p^r(\mathbf{x}) \nabla_{\mathbf{y}^T \mathbf{g}_r} k_{rg_r}(\mathbf{x}^T \mathbf{g}_r, \mathbf{y}^T \mathbf{g}_r) \\ &\quad + (\mathbf{r}^T \mathbf{g}_r)^2 \nabla_{\mathbf{x}^T \mathbf{g}_r, \mathbf{y}^T \mathbf{g}_r}^2 k_{rg_r}(\mathbf{x}^T \mathbf{g}_r, \mathbf{y}^T \mathbf{g}_r). \end{aligned} \quad (25)$$

Then we can compute the optimality w.r.t. test functions as an RKHS norm:

$$\begin{aligned} D_{rg_r}^2(q, p) &= \left(\sup_{\substack{h_{rg_r} \in \mathcal{H}_{rg_r} \\ \|h_{rg_r}\|_{\mathcal{H}_{rg_r}} \leq 1}} \mathbb{E}_q[s_p^r(\mathbf{x})h_{rg_r}(\mathbf{x}^T \mathbf{g}_r) \right. \\ &\quad \left. + \mathbf{r}^T \mathbf{g}_r \nabla_{\mathbf{x}^T \mathbf{g}_r} h_{rg_r}(\mathbf{x}^T \mathbf{g}_r)] \right)^2 \\ &= \|\mathbb{E}_q[\xi_{p,r,g_r}(\mathbf{x})]\|_{\mathcal{H}_{rg_r}}^2 = \mathbb{E}_{q(\mathbf{x})q(\mathbf{x}')}[\mu_{p,r,g_r}(\mathbf{x}, \mathbf{x}')] \end{aligned} \quad (26)$$

where \mathcal{H}_{rg_r} is the RKHS induced by the kernel k_{rg_r} . Therefore, the \max_{SSD-g} and \max_{SSD-rg} can be computed as

$$SK_{\max_{g_r}}(q, p) = \sum_{\mathbf{r} \in \mathcal{O}_r} \sup_{\mathbf{g}_r \in \mathbb{S}^{D-1}} D_{rg_r}^2(q, p) \quad (27)$$

and

$$SK_{\max_{r,g_r}}(q, p) = \sup_{\substack{\mathbf{g}_r \in \mathbb{S}^{D-1} \\ \mathbf{r} \in \mathbb{S}^{D-1}}} D_{rg_r}^2(q, p) \quad (28)$$

D. Goodness-of-fit test

In this section, we give an introduction to the GOF test. To be general, we focus on the $SKSD-rg$ ($SK_{rg_r} = \|\mathbb{E}_q[\xi_{p,r,g_r}(\mathbf{x})]\|_{\mathcal{H}_{rg_r}}^2$) as other related discrepancy can be easily derived from it. Assuming we have active slices \mathbf{r} and \mathbf{g}_r from algorithm 1. Thus, we can estimate SK_{rg_r} using the minimum variance U-statistics (Hoeffding, 1992; Serfling, 2009):

$$\widehat{SK}_{rg_r}(q, p) = \frac{1}{N(N-1)} \sum_{1 \leq i \neq j \leq N} \mu_{p,r,g_r}(\mathbf{x}_i, \mathbf{x}_j). \quad (29)$$

where $\mu_{\mathbf{x}, \mathbf{y}}$ is defined in Eq.25 which satisfies $\mathbb{E}_{q(\mathbf{x})q(\mathbf{x}')}[\mu_{p,r,g_r}(\mathbf{x}, \mathbf{x}')] = \|\mathbb{E}_q[\xi_{p,r,g_r}(\mathbf{x})]\|_{\mathcal{H}_{rg_r}}^2$, and \mathbf{x}, \mathbf{x}' are i.i.d. samples from q . With the help of the U-statistics, we characterize its asymptotic distribution.

Theorem 6. *Assume the conditions in theorem 1 are satisfied, we have the following:*

1. If $q \neq p$, then \widehat{SK}_{rg_r} is asymptotically normal. Particularly,

$$\sqrt{N}(\widehat{SK}_{rg_r} - SK_{rg_r}) \xrightarrow{d} \mathcal{N}(0, \sigma_h^2) \quad (30)$$

where $\sigma_h^2 = \text{var}_{\mathbf{x} \sim q}(\mathbb{E}_{\mathbf{x}' \sim q}[\mu_{p,r,g_r}(\mathbf{x}, \mathbf{x}')])$ and $\sigma_h \neq 0$

2. If $q = p$, we have a degenerated U-statistics with $\sigma_h = 0$ and

$$N\widehat{SK}_{rg_r} \xrightarrow{d} \sum_{j=1}^{\infty} c_j (Z_j^2 - 1) \quad (31)$$

where $\{Z_j\}$ are i.i.d standard Gaussian variables, and $\{c_j\}$ are the eigenvalues of the kernel $\mu_{p,r,g_r}(\mathbf{x}, \mathbf{x}')$ under $q(\mathbf{x})$. In other words, they are the solutions of $c_j \phi_j(\mathbf{x}) = \int_{\mathbf{x}'} \mu_{p,r,g_r}(\mathbf{x}, \mathbf{x}') \phi_j(\mathbf{x}') q(\mathbf{x}') d\mathbf{x}'$.

Proof. As the \widehat{SK}_{rg_r} is the second order U-statistic of SK_{rg_r} , thus, we can directly use the results from section 5.5.1 and 5.5.2 in (Serfling, 2009). \square

The above theorem indicates a well-defined asymptotic distribution for SK_{rg_r} , which allows us to use the following bootstrap method to estimate the rejection threshold (Huskova & Janssen, 1993; Arcones & Gine, 1992; Liu et al., 2016). The bootstrap samples can be computed as

$$\widehat{SK}_m^* = \sum_{1 \leq i \neq j \leq N} (w_i^m - \frac{1}{N})(w_j^m - \frac{1}{N}) \mu_{p,r,g_r}(\mathbf{x}_i, \mathbf{x}_j) \quad (32)$$

where $(w_1^m, \dots, w_N^m)_{m=1}^M$ are random weights drawn from multinomial distributions $\text{Multi}(N, \frac{1}{N}, \dots, \frac{1}{N})$. Now, we give the detailed algorithm for GOF test.

Algorithm 2 GOF test with active slices

Input: Samples $\mathbf{x} \sim q$, density p , kernel k_{rg_r} , active slices \mathbf{r}, \mathbf{g}_r , significance level α , and bootstrap sample size M .

Hypothesis: $H_0: p = q$ v.s. $H_1: p \neq q$

Computing U-statistics \widehat{SK}_{rg_r} using Eq.29

Generate M bootstrap samples $\{\widehat{SK}_m^*\}_{m=1}^M$ using Eq.32

Reject null hypothesis H_0 if the proportion of $\widehat{SK}_m^* > \widehat{SK}_{rg_r}$ is less than α

E. Relaxing constraints for kernelized SSD family

E.1. Validity w.r.t \mathbf{r}, \mathbf{g}_r

The key to this proof is to prove the real analyticity of SK_{g_r} (or S_{rg_r}) to slices \mathbf{r} and \mathbf{g}_r . Therefore, let's first give a definition of multivariate real analytic function.

Definition E.1 (Real analytic function). *A function $f: \mathcal{U} \rightarrow \mathbb{R}$ is real analytic if for each $\mathbf{c} \in \mathcal{U}$, there is a power series as in the form*

$$f(\mathbf{x}) = \sum_{\kappa \in \mathbb{N}_0^n} \alpha_{\kappa} (\mathbf{x} - \mathbf{c})^{\kappa}$$

for some choice of $(\alpha_\kappa)_{\kappa \in \mathbb{N}_0^D} \subset \mathbb{R}$ and all \mathbf{x} in a neighbourhood of \mathbf{c} , and this power series converges absolutely. Namely,

$$\sum_{\kappa \in \mathbb{N}_0^D} |\alpha_\kappa| |(\mathbf{x} - \mathbf{c})^\kappa| < \infty$$

where $\mathbb{N}_0 = \{0, 1, \dots\}$ denotes non-negative integers, $\kappa = (\kappa_1, \dots, \kappa_D)$ are called multiindex, and we define $\mathbf{x}^\kappa = x_1^{\kappa_1} \dots x_D^{\kappa_D}$.

Now, we introduce a useful lemma showing that composition of real analytic function is also real analytic.

Lemma 1 (Composition of real analytic function). *Let $\mathcal{U} \subset \mathbb{R}^n$ and $\mathcal{V} \subset \mathbb{R}^m$ be open, and let $\mathbf{f} : \mathcal{U} \rightarrow \mathcal{V}$ and $\mathbf{g} : \mathcal{V} \rightarrow \mathbb{R}^p$ be real analytic. Then $\mathbf{g} \circ \mathbf{f} : \mathcal{U} \rightarrow \mathbb{R}^p$ is real analytic.*

Especially, the real analyticity is not only preserved by function composition, it is also closed under most of the simple operations: addition, multiplication, division (assuming denominator is non-zero), etc. Now we can prove the main proposition to show that the *SKSD-rg* (SK_{r, g_r}) is real analytic w.r.t both \mathbf{g}_r and \mathbf{r} . In the following, we assume the $\mathbf{r}, \mathbf{g}_r \in \mathbb{R}^D$.

Proposition 2 (*SKSD-g* is real analytic). *Assume assumption 1-4, 7, and 8 are satisfied, further we let $\mathbf{g}_r \in \mathbb{R}^D$, then *SKSD-g* (SK_{g_r}) is real analytic w.r.t \mathbf{g}_r and SK_{r, g_r} is real analytic to both $\mathbf{r} \in \mathbb{R}^D$ and \mathbf{g}_r .*

Proof. First, let's focus on the real analyticity w.r.t. \mathbf{g}_r . We re-write the *SKSD-g* as the following:

$$\begin{aligned} SK_{g_r} &= \sum_{\mathbf{r} \in O_r} \|\xi_{p, r, g_r}(\mathbf{x})\|_{\mathcal{H}_{r, g_r}}^2 \\ &= \sum_{\mathbf{r} \in O_r} \langle \mathbb{E}_{\mathbf{q}}[(s_p^r(\mathbf{x}) - s_q^r(\mathbf{x})) k_{r, g_r}(\mathbf{x}^T \mathbf{g}_r, \cdot)], \\ &\quad \underbrace{f_r^*(\mathbf{x})}_{f_r^*(\mathbf{x})} \rangle, \\ &= \mathbb{E}_{\mathbf{q}}[(s_p^r(\mathbf{x}) - s_q^r(\mathbf{x})) k_{r, g_r}(\mathbf{x}^T \mathbf{g}_r, \cdot)]_{\mathcal{H}_{r, g_r}} \\ &= \sum_{\mathbf{r} \in O_r} \mathbb{E}_{\mathbf{x}, \mathbf{x}'} [f_r^*(\mathbf{x}) k_{r, g_r}(\mathbf{x}^T \mathbf{g}_r, \mathbf{x}'^T \mathbf{g}_r) f_r^*(\mathbf{x}')] \end{aligned}$$

The second equality is from the definition of RKHS norm $\|\cdot\|_{\mathcal{H}_{r, g_r}}$ and Stein identity. We can observe that \mathbf{g}_r appears inside the kernel k_{r, g_r} in the form of $\mathbf{x}^T \mathbf{g}_r$. So in order to use the function composition lemma (lemma 1), we need to first show that for any given \mathbf{x} , $\mathbf{x}^T \mathbf{g}_r$ is real analytic. By definition of real analytic function, we need a center point $\mathbf{c} \in \mathbb{R}^D$, and \mathbf{g}_r in the neighborhood of \mathbf{c} (i.e. $|\mathbf{g}_r - \mathbf{c}| < R_c$). Then, we define the power series as

$$h_x(\mathbf{g}_r) = \sum_{\kappa_1=0}^{\infty} \dots \sum_{\kappa_D=0}^{\infty} \frac{(g_{r1} - c_1)^{\kappa_1} \dots (g_{rD} - c_D)^{\kappa_D}}{\kappa_1! \dots \kappa_D!} \alpha_{\{\kappa_i\}_i^D}$$

with the following coefficient

$$\begin{cases} \alpha_{\{\kappa_i\}_i^D} = 0 & \text{if } \sum_i \kappa_i > 1 \\ \alpha_{\{\kappa_i\}_i^D} = x_i & \text{if } \kappa_i = 1, \sum_i \kappa_i = 1 \\ \alpha_{\{\kappa_i\}_i^D} = \mathbf{c}^T \mathbf{x} & \text{if } \sum_i \kappa_i = 0 \end{cases}$$

Then, by substitution, we have

$$h_x(\mathbf{g}) = \sum_{d=1}^D (g_d - c_d) x_d + \mathbf{c}^T \mathbf{x} \quad (33)$$

$$= \mathbf{x}^T \mathbf{g} \quad (34)$$

which converges with radius of convergence $R_c = \infty$. From assumption 8, we know the kernel $k_{r, g_r}(\mathbf{x}^T \mathbf{g}_r, \mathbf{x}'^T \mathbf{g}_r) = \phi((\mathbf{x} - \mathbf{x}')^T \mathbf{g}_r)$ is translation invariant and real analytic. Thus, from lemma 1, we know $k_{r, g_r}(\mathbf{x}^T \mathbf{g}_r, \mathbf{x}'^T \mathbf{g}_r)$ is real analytic to \mathbf{g}_r with radius of convergence R_k (R_k is determined by the form of the kernel function). This means we can use a power series to represents this kernel w.r.t. \mathbf{g}_r inside some neighborhood define around center point. Specifically, for a central point $\mathbf{c} \in \mathbb{R}^D$ and any \mathbf{g}_r satisfying $|\mathbf{g}_r - \mathbf{c}| < R_k$, we have

$$k_{r, g_r}(\mathbf{x}^T \mathbf{g}_r, \mathbf{x}'^T \mathbf{g}_r) = \sum_{\kappa \in \mathbb{N}_0^D} \alpha_\kappa(\mathbf{x}, \mathbf{x}') (\mathbf{g}_r - \mathbf{c})^\kappa$$

where this series converges absolutely. We substitute it into SK_{g_r} .

$$\begin{aligned} SK_{g_r} &= \sum_{\mathbf{r} \in O_r} \mathbb{E}_{\mathbf{x}, \mathbf{x}'} [f_r^*(\mathbf{x}) k_{r, g_r}(\mathbf{x}^T \mathbf{g}_r, \mathbf{x}'^T \mathbf{g}_r) f_r^*(\mathbf{x}')] \\ &= \sum_{\mathbf{r} \in O_r} \mathbb{E}_{\mathbf{x}, \mathbf{x}'} [f_r^*(\mathbf{x}) \sum_{\kappa \in \mathbb{N}_0^D} \alpha_\kappa(\mathbf{x}, \mathbf{x}') (\mathbf{g}_r - \mathbf{c})^\kappa f_r^*(\mathbf{x}')] \\ &= \sum_{\mathbf{r} \in O_r} \sum_{\kappa \in \mathbb{N}_0^D} \mathbb{E}_{\mathbf{x}, \mathbf{x}'} [\alpha_\kappa(\mathbf{x}, \mathbf{x}') f_r^*(\mathbf{x}) f_r^*(\mathbf{x}')] (\mathbf{g}_r - \mathbf{c})^\kappa \end{aligned}$$

which also converges absolutely with radius of convergence R_k . The third equality is from the Fubini's theorem. The conditions of Fubini's theorem can be verified by fact that f_r^* is square integrable (assumption 2), and the power series of k_{r, g_r} converges absolutely. Thus, by definition of real analytic function, *SKSD-g* is real analytic w.r.t each \mathbf{g}_r . This also implies *SKSD-rg* (SK_{r, g_r}) is real analytic w.r.t. \mathbf{g}_r (because SK_{r, g_r} is just SK_{g_r} without summation over O_r).

For the real analyticity w.r.t \mathbf{r} , the proof is almost the same. The inner product $s_p^r(\mathbf{x}) - s_q^r(\mathbf{x})$ is real analytic w.r.t \mathbf{r} obviously for given \mathbf{x} . We also use the fact that real analyticity is preserved under multiplication of two real analytic functions. In addition, note that $k_{r, g_r}(\mathbf{x}^T \mathbf{g}_r, \mathbf{x}'^T \mathbf{g}_r)$ act as a constant w.r.t. \mathbf{r} , we can directly apply the Fubini's theorem again to form a power series w.r.t. \mathbf{r} with absolute convergence. Thus, SK_{r, g_r} is real analytic w.r.t. \mathbf{r} for any \mathbf{g}_r . Thus, SK_{r, g_r} is real analytic to both \mathbf{r} and \mathbf{g}_r . \square

Next, we introduce an important property of real analytic function:

Lemma 2 (Zero Set Theorem(Mityagin, 2015)). *Let $f(\mathbf{x})$ be a real analytic function on (a connected open domain \mathcal{U} of) \mathbb{R}^d . If f is not identically 0, then its zero set*

$$S(f) := \{\mathbf{x} \in \mathcal{U} | f(\mathbf{x}) = 0\}$$

has a measure 0, i.e. $mes_d S(f) = 0$

With the help from the zero-set theorem, we can prove the validity of SK_{g_r} (or $SK_{r_{g_r}}$) with finite random slices \mathbf{g}_r (and \mathbf{r}).

Proof of theorem 1

Proof. We first deal with the validity of \mathbf{g}_r with fixed orthogonal basis O_r . It is trivial that when $p = q$, $SK_{g_r} = 0$ identically. Now, assume $p \neq q$, then, from the theorem 3 in (Gong et al., 2021), the orthogonal SKSD (Eq.35) is a valid discrepancy. Namely, we have

$$\sum_{\mathbf{r} \in O_r} \int q_{g_r}(\mathbf{g}_r) \|\mathbb{E}_q[\xi_{p,r,g_r}(\mathbf{x})]\|_{\mathcal{H}_{r,g_r}}^2 > 0 \quad (35)$$

We should note that the distribution q_{g_r} is originally defined on \mathbb{S}^{D-1} . But, we can easily generalize it to larger spaces. As for $\mathbf{g}_r \in \mathbb{R}^D$, we can always write $\mathbf{g}_r = c\mathbf{g}'_r$, where $\mathbf{g}'_r \in \mathbb{S}^{D-1}$, and $c \geq 0$. As the domain for \mathbf{g}_r is \mathbb{R}^D , the \mathbf{g}_r can represents all possible directions. Thus, we can follow the same proof logic as theorem 3 in (Gong et al., 2021) to show the corresponding discrepancy is greater than 0 when $p \neq q$.

Therefore, Eq.35 represents there exists a $\mathbf{r} \in O_r$ such that $\|\mathbb{E}_q[\xi_{p,r,g_r}(\mathbf{x})]\|_{\mathcal{H}_{r,g_r}}^2 > 0$ for a set of \mathbf{g}_r with non-zero measure. Namely, $\|\mathbb{E}_q[\xi_{p,r,g_r}(\mathbf{x})]\|_{\mathcal{H}_{r,g_r}}^2$ is not 0 identically. Thus, from the proposition 2 and lemma 2, the set of \mathbf{g}_r that make $\|\mathbb{E}_q[\xi_{p,r,g_r}(\mathbf{x})]\|_{\mathcal{H}_{r,g_r}}^2 = 0$ has a 0 measure. Then, if \mathbf{g}_r is sampled from some distribution η_g with density supported on \mathbb{R}^D (e.g. Gaussian distribution), we have

$$SK_{g_r} = \sum_{\mathbf{r} \in O_r} \|\mathbb{E}_q[\xi_{p,r,g_r}(\mathbf{x})]\|_{\mathcal{H}_{r,g_r}}^2 > 0$$

almost surely.

Now, we show that $SK_{r_{g_r}}$ is also a valid discrepancy with $\mathbf{r} \sim \eta_r$. First, due to the validity of *integrated SKSD*, we have

$$\int q_r(\mathbf{r}) \int q_{g_r}(\mathbf{g}_r) \|\mathbb{E}_q[\xi_{p,r,g_r}(\mathbf{x})]\|_{\mathcal{H}_{r,g_r}}^2 d\mathbf{g}_r d\mathbf{r} > 0 \quad (36)$$

Due to the real analyticity of $SK_{r_{g_r}}$ ($\|\mathbb{E}_q[\xi_{p,r,g_r}(\mathbf{x})]\|_{\mathcal{H}_{r,g_r}}^2$) w.r.t \mathbf{r} , we can easily show that

$$\int q_{g_r}(\mathbf{g}_r) \|\mathbb{E}_q[\xi_{p,r,g_r}(\mathbf{x})]\|_{\mathcal{H}_{r,g_r}}^2 d\mathbf{g}_r$$

is real analytic to \mathbf{r} and it is not 0 identically. Thus, by lemma 2, for $\mathbf{r} \sim \eta_r$, we have

$$\int q_{g_r}(\mathbf{g}_r) \|\mathbb{E}_q[\xi_{p,r,g_r}(\mathbf{x})]\|_{\mathcal{H}_{r,g_r}}^2 d\mathbf{g}_r > 0$$

Namely, $\|\mathbb{E}_q[\xi_{p,r,g_r}(\mathbf{x})]\|_{\mathcal{H}_{r,g_r}}^2 > 0$ for a set of \mathbf{g}_r with non-zero measure. In the beginning of the proof, we show that this set of \mathbf{g}_r is almost everywhere in \mathbb{R}^D due to its real analyticity. Namely, $\|\mathbb{E}_q[\xi_{p,r,g_r}(\mathbf{x})]\|_{\mathcal{H}_{r,g_r}}^2 > 0$ for $\mathbf{r} \sim \eta_r$ and $\mathbf{g}_r \sim \eta_g$ if $p \neq q$. Thus, we can conclude that for $SK_{r_{g_r}} = 0$ if and only if $p = q$ almost surely for $\mathbf{r} \sim \eta_r$ and $\mathbf{g}_r \sim \eta_g$. \square

Corollary 6.1 (Normalizing \mathbf{g}_r). *Assume the conditions in theorem 1 are satisfied, then the following operations do not violate the validity of SKSD-rg $SK_{r_{g_r}}$. (1) For $\mathbf{g}'_r, \mathbf{r}' \in \mathbb{S}^{D-1}$, we define $\mathbf{g}_r = \mathbf{g}'_r + \gamma_g$ and $\mathbf{r} = \mathbf{r}' + \gamma_r$, where γ_r, γ_g are the noise from Gaussian distribution. (2) Define $\tilde{\mathbf{g}}_r = c_g \times \mathbf{g}_r$ and $\tilde{\mathbf{r}} = c_r \times \mathbf{r}$, where $\tilde{\mathbf{g}}_r, \tilde{\mathbf{r}}$ are unit vectors and $c_r, c_g > 0$. The resulting active slices $\tilde{\mathbf{r}}$ and $\tilde{\mathbf{g}}_r$ do not violate the validity of $SK_{r_{g_r}}$.*

Proof. From the theorem 1 with \mathbf{g}_r, \mathbf{r} , when $p \neq q$, we have

$$\begin{aligned} SK_{r_{g_r}} &= \|\mathbb{E}_q[\xi_{p,r,g_r}(\mathbf{x})]\|_{\mathcal{H}_{r,g_r}}^2 \\ &= \mathbb{E}_{\mathbf{x}, \mathbf{x}'} [f_r^*(\mathbf{x}) k_{r_{g_r}}(\mathbf{x}^T \mathbf{g}_r, \mathbf{x}'^T \mathbf{g}_r) f_r^*(\mathbf{x}')] \\ &= \mathbb{E}_{\mathbf{x}, \mathbf{x}'} [c_r^2 f_r^*(\mathbf{x}) k_{r_{g_r}}(c\mathbf{x}^T \tilde{\mathbf{g}}_r, c\mathbf{x}'^T \tilde{\mathbf{g}}_r) f_r^*(\mathbf{x}')] > 0 \end{aligned}$$

From the assumption 8 that $k_{r_{g_r}}(c\mathbf{x}^T \tilde{\mathbf{g}}_r, c\mathbf{x}'^T \tilde{\mathbf{g}}_r) = k'_{r_{g_r}}(\mathbf{x}^T \tilde{\mathbf{g}}_r, \mathbf{x}'^T \tilde{\mathbf{g}}_r)$. So this is equivalent to the *SKSD-rg* defined with a new c_0 -universal kernel $k'_{r_{g_r}}$ and $\tilde{\mathbf{g}}_r, \tilde{\mathbf{r}} \in \mathbb{S}^{D-1}$. Thus, the corresponding *maxSKSD-rg* with $\tilde{\mathbf{g}}_r, \tilde{\mathbf{r}} \in \mathbb{S}^{D-1}$ is a valid discrepancy almost surely. \square

E.2. Relationship between SSD and SKSD

Before we jump into the details, the supremum of $h_{r_{g_r}}$ in $S_{r_{g_r}}$ hinders the further analysis. The following proposition analytically gives the optimal form of $h_{r_{g_r}}$.

Proposition 3 (Optimal test function given \mathbf{r}, \mathbf{g}_r). *Assume assumptions 1-4 and given directions \mathbf{r}, \mathbf{g}_r . Assume an arbitrary orthogonal matrix $\mathbf{G}_r = [\mathbf{a}_1, \dots, \mathbf{a}_D]^T$ where $\mathbf{a}_i \in \mathbb{S}^{D \times 1}$ and $\mathbf{a}_d = \mathbf{g}_r$. Denote $\mathbf{x} \sim q$ and $\mathbf{y} = \mathbf{G}_r \mathbf{x}$ which is also a random variable with the induced distribution q_{G_r} . Then, the optimal test function for $S_{r_{g_r}}$ is*

$$h_{r_{g_r}}^*(\mathbf{x}^T \mathbf{g}_r) \propto \mathbb{E}_{q_{G_r}(\mathbf{y}_{-d} | y_d)} [(s_p^r(\mathbf{G}_r^{-1} \mathbf{y}) - s_q^r(\mathbf{G}_r^{-1} \mathbf{y}))] \quad (37)$$

where $y_d = \mathbf{x}^T \mathbf{g}_r$ and \mathbf{y}_{-d} contains other \mathbf{y} elements.

Proof of proposition 3

Proof. We consider the $SSD\text{-}rg$ (S_{r,g_r}) without the optimal test function:

$$\mathbb{E}_q[s_p^r(\mathbf{x})h_{r,g_r}(\mathbf{x}^T \mathbf{g}_r) + \mathbf{r}^T \mathbf{g}_r \nabla_{\mathbf{x}^T \mathbf{g}_r} h_{r,g_r}(\mathbf{x}^T \mathbf{g}_r)] \quad (38)$$

From the Stein identity (Eq.17), we can let $\mathbf{f}(\mathbf{x}) = [r_1 h_{r,g_r}(\mathbf{x}^T \mathbf{g}_r), r_2 h_{r,g_r}(\mathbf{x}^T \mathbf{g}_r), \dots, r_D h_{r,g_r}(\mathbf{x}^T \mathbf{g}_r)]^T$ and then take the trace. Thus, we have

$$\mathbb{E}_q[s_p^r(\mathbf{x})h_{r,g_r}(\mathbf{x}^T \mathbf{g}_r)] = \mathbb{E}_q[\mathbf{r}^T \mathbf{g}_r \nabla_{\mathbf{x}^T \mathbf{g}_r} h_{r,g_r}(\mathbf{x}^T \mathbf{g}_r)]$$

Substitute it into Eq.38 and change the variable to $\mathbf{y} = \mathbf{G}_r \mathbf{x}$, we have

$$\begin{aligned} & \mathbb{E}_q[(s_p^r(\mathbf{x}) - s_q^r(\mathbf{x}))h_{r,g_r}(\mathbf{x}^T \mathbf{g}_r)] \\ &= \int q_{G_r}(y_d, \mathbf{y}_{-d}) \underbrace{(s_p^r(\mathbf{G}_r^{-1} \mathbf{y}) - s_q^r(\mathbf{G}_r^{-1} \mathbf{y}))}_{f_r^*(\mathbf{G}_r^{-1} \mathbf{y})} h_{r,g_r}(y_d) d\mathbf{y} \\ &= \int q_{G_r}(y_d) \int q_{G_r}(\mathbf{y}_{-d}|y_d) \underbrace{f_r^*(\mathbf{G}_r^{-1} \mathbf{y})}_{h_{r,g_r}^*(y_d)} d\mathbf{y}_{-d} h_{r,g_r}(y_d) dy_d \\ &\leq \sqrt{\mathbb{E}_{q_{G_r}(y_d)}[h_{r,g_r}^*(y_d)^2]} \sqrt{\mathbb{E}_{q_{G_r}(y_d)}[h_{r,g_r}(y_d)^2]} \end{aligned}$$

where the last inequality is from Cauchy-Schwarz inequality, where the equality holds when

$$\begin{aligned} h_{r,g_r}(y_d) &\propto h_{r,g_r}^*(y_d) \\ &= \mathbb{E}_{q_{G_r}(\mathbf{y}_{-d}|y_d)} [(s_p^r(\mathbf{G}_r^{-1} \mathbf{y}) - s_q^r(\mathbf{G}_r^{-1} \mathbf{y}))] \end{aligned}$$

where $y_d = \mathbf{x}^T \mathbf{g}_r$. \square

Proof of theorem 2

Proof. Let's first re-write of S_{r,g_r} and SK_{r,g_r} .

$$\begin{aligned} S_{r,g_r} &= \sup_{h_{r,g_r} \in \mathcal{F}_q} \mathbb{E}_q[(s_p^r(\mathbf{y}) - s_q^r(\mathbf{x}))h_{r,g_r}(\mathbf{x}^T \mathbf{g}_r)] \\ &= \mathbb{E}_{q_{G_r}(y_d)} \left[\int q_{G_r}(\mathbf{y}_{-d}|y_d) \underbrace{(s_p^r(\mathbf{G}_r^{-1} \mathbf{y}) - s_q^r(\mathbf{G}_r^{-1} \mathbf{y}))}_{h_{r,g_r}^*(y_d)} d\mathbf{y}_{-d} \right] \\ &\times h_{r,g_r}^*(y_d) \\ &= \mathbb{E}_{q_{G_r}(y_d)} [h_{r,g_r}^*(y_d)^2] \end{aligned}$$

where the second equality is from proposition 3.

$$SK_{r,g_r} = \langle \mathbb{E}_q[\xi_{p,r,g_r}(\mathbf{x})], \mathbb{E}_q[\xi_{p,r,g_r}(\mathbf{x})] \rangle_{\mathcal{H}_k}$$

where $\xi_{p,r,g_r}(\mathbf{x}, \cdot)$ is defined in Eq.5, and $\langle \cdot, \cdot \rangle_{\mathcal{H}_{r,g_r}}$ is the RKHS inner product induced by kernel k_{r,g_r} . By simple

algebraic manipulation and Stein identity (Eq.17), we have

$$\begin{aligned} & \mathbb{E}_q[\xi_{p,r,g_r}(\mathbf{x}, \cdot)] \\ &= \mathbb{E}_q[(s_p^r(\mathbf{x}) - s_q^r(\mathbf{x}))k_{r,g_r}(\mathbf{x}^T \mathbf{g}_r, \cdot)] \\ &= \mathbb{E}_{q_{G_r}(y_d)} \left[\int q_{G_r}(\mathbf{y}_{-d}|y_d) \underbrace{(s_p^r(\mathbf{G}_r^{-1} \mathbf{y}) - s_q^r(\mathbf{G}_r^{-1} \mathbf{y}))}_{h_{r,g_r}^*(y_d)} d\mathbf{y}_{-d} \right] \\ &\times k_{r,g_r}(y_d, \cdot) \\ &= \mathbb{E}_{q_{G_r}(y_d)} [h_{r,g_r}^*(y_d)k_{r,g_r}(y_d, \cdot)] \end{aligned}$$

Thus, we have

$$\begin{aligned} & SK_{r,g_r} \\ &= \mathbb{E}_{y_d, y'_d \sim q_{G_r}(y_d)} [h_{r,g_r}^*(y_d)k_{r,g_r}(y_d, y'_d)h_{r,g_r}^*(y'_d)] \\ &\leq \sqrt{\mathbb{E}_{y_d, y'_d} [k_{r,g_r}(y_d, y'_d)^2]} \sqrt{\mathbb{E}_{y_d} [h_{r,g_r}^*(y_d)^2]} \sqrt{\mathbb{E}_{y'_d} [h_{r,g_r}^*(y'_d)^2]} \\ &= M S_{r,g_r}^* \end{aligned}$$

where constant M is from the bounded kernel assumption, and the inequality is from Cauchy-Schwarz inequality. Without the loss of generality, we can set $M = 1$. For other value of $M > 0$, one can always set the optimal test function (h_{r,g_r}^*) for $SSD\text{-}rg$ with coefficient M . The the new $SSD\text{-}g$ will be M multiplied by the original $SSD\text{-}rg$ with $M = 1$.

Thus, $SSD\text{-}rg$ is an upper bound for $SKSD\text{-}rg$. From the assumption 1, we know that the induced set $\mathcal{K} = \{y \in \mathbb{R} | y = \mathbf{x}^T \mathbf{g}, ||g|| = 1, \mathbf{x} \in \mathcal{X}\}$ is LCH, and the kernel $k_{r,g_r} : \mathcal{K} \times \mathcal{K} \rightarrow \mathbb{R}$ is c_0 -universal. Then, from (Sriperumbudur et al., 2011), c_0 -universal implies L_p -universal. Namely, the induced RKHS \mathcal{H}_{r,g_r} is dense in $L^p(\mathcal{K}; \mu)$ with all Borel probability measure μ w.r.t. p -norm, defined as

$$||f||_p = \left(\int |f(\mathbf{x})|^p d\mu(\mathbf{x}) \right)^{\frac{1}{p}}$$

Now, from the assumption 4, we know $h_{r,g_r}^*(y_d)$ is bounded for all possible \mathbf{g}_r , we have

$$\int q_{G_r}(y_d) |h_{r,g_r}^*(y_d)|^2 dy_d < \infty$$

This means $h_{r,g_r}^* \in L^2(\mathcal{K}, \mu_{G_r})$, where μ_{G_r} is the probability measure with density $q_{G_r}(y_d)$

From the L_p -universality, there exists a function $\widetilde{h_{r,g_r}^*} \in \mathcal{H}_{r,g_r}$, such that for any given $\epsilon > 0$,

$$||h_{r,g_r}^* - \widetilde{h_{r,g_r}^*}||_2 < \epsilon$$

Let's define \widetilde{SK}_{r,g_r} is the $SKSD\text{-}rg$ with the specific kernelized test function $\widetilde{h_{r,g_r}^*}$, and from the optimality of $SKSD\text{-}rg$, we have

$$SK_{r,g_r} \geq \widetilde{SK}_{r,g_r}$$

Therefore, we have

$$\begin{aligned}
 0 &\leq S_{r_{g_r}} - SK_{r_{g_r}} \\
 &\leq S_{r_{g_r}} - \widetilde{SK}_{r_{g_r}} \\
 &= \mathbb{E}_q[(s_p^r(\mathbf{x}) - s_q^r(\mathbf{x}))(h_{r_{g_r}}^*(\mathbf{x}^T \mathbf{g}_r) - \widetilde{h_{r_{g_r}}^*}(\mathbf{x}^T \mathbf{g}_r))] \\
 &\leq \underbrace{\sqrt{\mathbb{E}_q[(s_p^r(\mathbf{x}) - s_q^r(\mathbf{x}))^2]}}_{C_r} \\
 &\quad \times \sqrt{\mathbb{E}_q[(h_{r_{g_r}}^*(\mathbf{x}^T \mathbf{g}_r) - \widetilde{h_{r_{g_r}}^*}(\mathbf{x}^T \mathbf{g}_r))^2]} \\
 &= C_r \sqrt{\int q_{G_r}(y_d, \mathbf{y}_{-d})(h_{r_{g_r}}^*(y_d) - \widetilde{h_{r_{g_r}}^*}(y_d))^2 d\mathbf{y}} \\
 &= C_r \|h_{r_{g_r}}^* - \widetilde{h_{r_{g_r}}^*}\|_2 < C_r \epsilon
 \end{aligned}$$

From assumption 2, we know $s_p^r(\mathbf{x}) - s_q^r(\mathbf{x})$ is square integrable for all possible \mathbf{r} . Therefore, let's define $C = \max_{\mathbf{r} \in \mathbb{S}^{D-1}} C_r$, then,

$$0 \leq S_{r_{g_r}} - SK_{r_{g_r}} < C \epsilon$$

□

F. Theory related to active slice g

F.1. Optimal test function for PSD

Proposition 4 (Optimality of PSD). *Assume the assumption 1 – 3 are satisfied, then the optimal test function for PSD given O_r is proportional to the projected score difference, i.e.*

$$f_r^*(\mathbf{x}) \propto (s_p^r(\mathbf{x}) - s_q^r(\mathbf{x})) \quad (39)$$

Thus,

$$PSD(q, p; O_r) = \sum_{\mathbf{r} \in O_r} \mathbb{E}_q[(s_p^r(\mathbf{x}) - s_q^r(\mathbf{x}))^2] \quad (40)$$

if the coefficient of f_r^* to be 1.

Proof. From the Stein identity (Eq.17), we can re-write the inner part of the supremum of Eq.7 as

$$\begin{aligned}
 &\mathbb{E}_q[s_p^r(\mathbf{x})f_r(\mathbf{x}) + \mathbf{r}^T \nabla_{\mathbf{x}} f_r(\mathbf{x})] \\
 &= \mathbb{E}_q[(s_p^r(\mathbf{x}) - s_q^r(\mathbf{x}))f_r(\mathbf{x})]
 \end{aligned}$$

Then, we can upper bound the PSD (Eq.7) as the following

$$\begin{aligned}
 &\sum_{\mathbf{r} \in O_r} \mathbb{E}_q[(s_p^r(\mathbf{x}) - s_q^r(\mathbf{x}))f_r(\mathbf{x})] \\
 &\leq \sum_{\mathbf{r} \in O_r} \sqrt{\mathbb{E}_q[(s_p^r(\mathbf{x}) - s_q^r(\mathbf{x}))^2]} \sqrt{\mathbb{E}_q[(f_r(\mathbf{x}))^2]}
 \end{aligned}$$

by Cauchy-Schwarz inequality. It is well-known that the equality holds when $f_r(\mathbf{x}) \propto (s_p^r(\mathbf{x}) - s_q^r(\mathbf{x}))$ □

F.2. Proof of Theorem 3

Proof. The key to this proof is to notice that $h_{r_{g_r}}^*$ is the conditional mean of f_r^* w.r.t. the transformed distribution q_{G_r} . By using the similar terminology of proposition 3, and let $s_p^r = s_p^r(\mathbf{x})$ for abbreviation. Then,

$$\begin{aligned}
 &\mathbb{E}_q[(s_p^r - s_q^r)f_r^*(\mathbf{x})] - \mathbb{E}_q[(s_p^r - s_q^r)h_{r_{g_r}}^*(\mathbf{x}^T \mathbf{g}_r)] \\
 &= \int q(\mathbf{x})[(s_p^r - s_q^r)^2 - (s_p^r - s_q^r)h_{r_{g_r}}^*(\mathbf{x}^T \mathbf{g}_r)]d\mathbf{x} \\
 &= \int q_{G_r}(y_d) \left[\int q_{G_r}(\mathbf{y}_{-d}|y_d)(s_p^r(\mathbf{G}_r^{-1}\mathbf{y}) - s_q^r(\mathbf{G}_r^{-1}\mathbf{y}))^2 d\mathbf{y}_{-d} \right. \\
 &\quad \left. - \int q_{G_r}(s_p^r(\mathbf{G}_r^{-1}\mathbf{y}) - s_q^r(\mathbf{G}_r^{-1}\mathbf{y}))d\mathbf{y}_{-d} \underbrace{h_{r_{g_r}}^*(y_d)}_{h_{r_{g_r}}^*(y_d)} \right] dy_d \\
 &= \int q_{G_r}(y_d) \left[\int q_{G_r}(\mathbf{y}_{-d}|y_d)(f_r^*(\mathbf{G}_r^{-1}\mathbf{y}) - h_{r_{g_r}}^*(y_d))^2 d\mathbf{y} \right. \\
 &\quad \left. - \mathbb{E}_q[(f_r^*(\mathbf{x}) - h_{r_{g_r}}^*(\mathbf{x}^T \mathbf{g}_r))^2] \right] dy_d \geq 0
 \end{aligned}$$

where the 3rd equality is due to the fact that $h_{r_{g_r}}^*$ is the conditional mean of f_r^* . Thus,

$$\begin{aligned}
 &PSD - S_{g_r} \\
 &= \sum_{\mathbf{r} \in O_r} \mathbb{E}_q[(s_p^r - s_q^r)f_r^*(\mathbf{x})] - \mathbb{E}_q[(s_p^r - s_q^r)h_{r_{g_r}}^*(\mathbf{x}^T \mathbf{g}_r)] \\
 &= \sum_{\mathbf{r} \in O_r} \mathbb{E}_q[(f_r^*(\mathbf{x}) - h_{r_{g_r}}^*(\mathbf{x}^T \mathbf{g}_r))] \geq 0
 \end{aligned}$$

□

F.3. Proof of Theorem 4

Before we give the details, we introduce the main inequality and its variant for the proof.

Lemma 3 (Poincaré Inequality). *For a probabilistic distribution p that satisfies assumption 5, for all locally Lipschitz function $f(\mathbf{x}) : \mathcal{X} \subseteq \mathbb{R}^D \rightarrow \mathbb{R}$, we have the following inequality*

$$\text{Var}_p(f(\mathbf{x})) \leq C_p \int p(\mathbf{x}) \|\nabla_{\mathbf{x}} f(\mathbf{x})\|^2 d\mathbf{x}$$

where C_p is called Poincaré constant that is only related to p .

One should note that the assumption of log concavity of p is a sufficient condition for Poincaré inequality, which means it may be applied to a broader class of distributions. But it is beyond the scope of this work.

Due to the form of optimal test functions of SSD - g , we need to deal with the transformed distribution q_{G_r} and its conditional expectations (see Eq.37). Unfortunately, the original form of Poincaré inequality cannot be applied. In the following, we introduce its variant called *subspace* Poincaré

inequality (Constantine et al., 2014; Zahm et al., 2020; Parante et al., 2020) to deal with the conditional expectation. But before that, we need to make sure the transformed distribution and its conditional density still satisfy the conditions of Poincaré inequality, i.e. log concavity.

Lemma 4 (Preservation of log concavity). *Assume distribution $q(\mathbf{x}) = \exp(-V(\mathbf{x}))$ is log-concave. With arbitrary orthogonal matrix \mathbf{G} and corresponding transformed distribution q_G , the conditional distribution $q_G(\mathbf{y}_{-d} | y_d)$ is also log-concave for all $d = 1, \dots, D$.*

Proof. Assume we have $\mathbf{y} = \mathbf{G}\mathbf{x}$. Thus, by change of variable formula, $q_G(\mathbf{y}) = q(\mathbf{x}) = q(\mathbf{G}^{-1}\mathbf{y}) = \exp(-V(\mathbf{G}^{-1}\mathbf{y}))$. Thus, the log conditional distribution

$$\log q_G(\mathbf{y}_{-d} | y_d) = -V(\mathbf{G}^{-1}\mathbf{y}) - \log q_G(y_d)$$

We inspect its Hessian w.r.t \mathbf{y}_{-d}

$$\begin{aligned} & \nabla_{\mathbf{y}_{-d}}^2 (V(\mathbf{G}^{-1}\mathbf{y}) + \log q_G(y_d)) \\ &= \nabla_{\mathbf{y}_{-d}}^2 (V(\mathbf{G}^{-1}\mathbf{y})) \\ &= \nabla_{\mathbf{y}_{-d}} (\mathbf{G}_{\setminus d} V'(\mathbf{G}^{-1}\mathbf{y})) \\ &= \mathbf{G}_{\setminus d} V''(\mathbf{G}^{-1}\mathbf{y}) \mathbf{G}_{\setminus d}^T \end{aligned}$$

where $\mathbf{G}_{\setminus d} = [\mathbf{g}_1, \dots, \mathbf{g}_{d-1}, \mathbf{g}_{d+1}, \dots, \mathbf{g}_D]^T$ and $V'(\mathbf{G}^{-1}\mathbf{y}) = \nabla_{\mathbf{G}^{-1}\mathbf{y}} V(\mathbf{G}^{-1}\mathbf{y})$. We already know that $V(\cdot)$ is a convex function. Thus, for all $\mathbf{u} \in \mathbb{R}^D$, $\mathbf{u}^T V''(\mathbf{x}) \mathbf{u} \geq 0$, therefore,

$$\mathbf{u}^T \mathbf{G}_{\setminus d} V''(\mathbf{G}^{-1}\mathbf{y}) \mathbf{G}_{\setminus d}^T \mathbf{u} = \mathbf{l}^T V''(\mathbf{G}^{-1}\mathbf{y}) \mathbf{l} \geq 0$$

where $\mathbf{l} = \mathbf{G}_{\setminus d}^T \mathbf{u}$. \square

Now, we can introduce the subspace Poincaré inequality

Lemma 5 (Poincaré inequality for conditional expectation). *Assume the assumption 2,4,5 are satisfied, with arbitrary orthogonal matrix \mathbf{G} , $\mathbf{y} = \mathbf{G}\mathbf{x}$ and $y_d = \mathbf{x}^T \mathbf{g}$, we have the following inequality*

$$\begin{aligned} & \int q_G(\mathbf{y}_{-d} | y_d) [f_r^*(\mathbf{G}^{-1}\mathbf{y}) - h_{r, \mathbf{g}_r}^*(y_d)]^2 d\mathbf{y}_{-d} \\ & \leq C_{y_d} \mathbb{E}_{q_G(\mathbf{y}_{-d} | y_d)} \left[\|\mathbf{G}_{\setminus d} \nabla f_r^*\|^2 \right] \end{aligned}$$

where C_{y_d} is the Poincaré constant, $\mathbf{G}_{\setminus d} = [\mathbf{a}_1, \dots, \mathbf{a}_{d-1}, \mathbf{a}_{d+1}, \dots, \mathbf{a}_D]^T$ is the orthogonal matrix \mathbf{G} excluding $\mathbf{a}_d = \mathbf{g}$ and f_r^* , h_{r, \mathbf{g}_r}^* are the optimal test functions defined in proposition 4, 3 respectively with coefficient 1.

Proof. From lemma 4, we know $q_G(\mathbf{y}_{-d} | y_d)$ is a log-concave distribution. Therefore, it satisfies the Poincaré

inequality (lemma.3). We have

$$\begin{aligned} & \int q_G(\mathbf{y}_{-d} | y_d) [f_r^*(\mathbf{G}^{-1}\mathbf{y}) - h_{r, \mathbf{g}_r}^*(y_d)]^2 d\mathbf{y}_{-d} \\ &= \text{Var}_{q_G(\mathbf{y}_{-d} | y_d)}(f_r^*(\mathbf{G}^{-1}\mathbf{y})) \\ & \leq C_{y_d} \int q_G(\mathbf{y}_{-d} | y_d) \|\nabla_{\mathbf{y}_{-d}} f_r^*(\mathbf{G}^{-1}\mathbf{y})\|^2 d\mathbf{y}_{-d} \\ &= C_{y_d} \int q_G(\mathbf{y}_{-d} | y_d) \|\mathbf{G}_{\setminus d} \nabla_{\mathbf{G}^{-1}\mathbf{y}} f_r^*(\mathbf{G}^{-1}\mathbf{y})\|^2 d\mathbf{y}_{-d} \end{aligned}$$

The first equality comes from the fact that $h_{r, \mathbf{g}_r}^*(y_d)$ is actually a conditional mean of $f_r^*(\mathbf{G}^{-1}\mathbf{y})$, and the inequality comes from the direct application of Poincaré inequality on $q_G(\mathbf{y}_{-d} | y_d)$ and $f_r^*(\mathbf{G}^{-1}\mathbf{y})$. \square

With the above tools, it is now easy to prove theorem 4.

Theorem 4

Proof. We can re-write the inner part of controlled approximation (Eq.9) in the following:

$$\begin{aligned} & \int q_{G_r}(y_d, \mathbf{y}_{-d}) [f_r^*(\mathbf{G}_r^{-1}\mathbf{y}) - h_{r, \mathbf{g}_r}^*(y_d)]^2 d\mathbf{y} \\ &= \int q_{G_r}(y_d) \mathbb{E}_{q_{G_r}(\mathbf{y}_{-d} | y_d)} [(f_r^*(\mathbf{G}_r^{-1}\mathbf{y}) - h_{r, \mathbf{g}_r}^*(y_d))^2] d\mathbf{y} \\ & \leq \int q_{G_r}(y_d, \mathbf{y}_{-d}) C_{y_d} \|\mathbf{G}_{r \setminus d} \nabla f_r^*\|^2 d\mathbf{y} \\ & \leq C_{sup} \int q_{G_r}(y_d, \mathbf{y}_{-d}) \|\mathbf{G}_{r \setminus d} \nabla f_r^*\|^2 d\mathbf{y} \\ &= C_{sup} \int q(\mathbf{x}) \text{tr} \left[(\mathbf{G}_{r \setminus d} \nabla f_r^*) (\mathbf{G}_{r \setminus d} \nabla f_r^*)^T \right] d\mathbf{x} \\ &= C_{sup} \text{tr} \left[\mathbf{G}_{r \setminus d} \mathbf{H}_r \mathbf{G}_{r \setminus d}^T \right] \end{aligned}$$

where the first inequality is directly from lemma 5 and the second inequality is from the definition of C_{sup} .

To minimize this upper bound, we can directly use the theorem 2.1 (Sameh & Tong, 2000) by setting $B = I$ and $\mathbf{X} = \mathbf{G}_{r \setminus d}^T$. Therefore, we only need to check if $\mathbf{G}_{r \setminus d} \mathbf{G}_{r \setminus d}^T = I$. This is trivial as \mathbf{G}_r is an orthogonal matrix. Thus, the proof is complete. \square

G. Theory related to active slice r

G.1. Proof of proposition 1

First, from the theorem 3, we have

$$\text{PSD}_r \geq S_{r, \mathbf{g}}$$

Thus, we can establish the following lower bound

$$\begin{aligned} & S_{r_1, g_{r_1}} - S_{r_2, g_{r_2}} \\ & \geq S_{r_1, g_{r_1}} - \text{PSD}_{r_2} \\ & = \underbrace{S_{r_1, g_{r_1}} - \text{PSD}_{r_1}}_{\text{controlled approximation}} + \text{PSD}_{r_1} - \text{PSD}_{r_2} \end{aligned}$$

Thus, from theorem 4, we can obtain

$$\begin{aligned} & S_{r_1, g_{r_1}} - \text{PSD}_{r_1} \\ & = -\mathbb{E}_q \left[(f_{r_1}^*(\mathbf{x}) - h_{r_1, g_{r_1}}^*(\mathbf{x}^T \mathbf{g}_{r_1}))^2 \right] \\ & \geq -C_{\text{sup}} \text{tr}(\mathbf{G}_{r_1} \mathbf{d} \mathbf{H}_{r_1} \mathbf{G}_{r_1}^T \mathbf{d}) \\ & = -C_{\text{sup}} \text{tr}(\mathbf{H}) + \underbrace{\mathbf{g}_{r_1}^T \mathbf{H}_{r_1} \mathbf{g}_{r_1}}_{\geq 0} \\ & \geq -C_{\text{sup}} \text{tr}(\mathbf{H}_{r_1}) \end{aligned}$$

where the first inequality is from the upper bound of controlled approximation (theorem 4) and $\mathbf{g}_{r_1}^T \mathbf{H}_{r_1} \mathbf{g}_{r_1} \geq 0$ is due to the positive semi-definiteness of \mathbf{H}_{r_1} . Assume we have an orthogonal basis O_{r_1} that contains \mathbf{r}_1 , thus, for each $\mathbf{r} \in O_{r_1}$, we have $\text{tr}(\mathbf{H}_r) \geq 0$. Then, we can show

$$\begin{aligned} \text{tr}(\mathbf{H}_{r_1}) & \leq \sum_{\mathbf{r} \in O_{r_1}} \text{tr}(\mathbf{H}_r) \\ & = \sum_{\mathbf{r} \in O_{r_1}} \text{tr}(\mathbb{E}_q[\nabla_{\mathbf{x}} \mathbf{f}^*(\mathbf{x}) \mathbf{r} \mathbf{r}^T \nabla_{\mathbf{x}} \mathbf{f}^*(\mathbf{x})^T]) \\ & = \text{tr}(\mathbb{E}_q[\nabla_{\mathbf{x}} \mathbf{f}^*(\mathbf{x}) \sum_{\mathbf{r} \in O_{r_1}} \mathbf{r} \mathbf{r}^T \nabla_{\mathbf{x}} \mathbf{f}^*(\mathbf{x})^T]) \\ & = \text{tr}(\mathbb{E}_q[\nabla_{\mathbf{x}} \mathbf{f}^*(\mathbf{x}) \nabla_{\mathbf{x}} \mathbf{f}^*(\mathbf{x})^T]) \\ & = \sum_{i=1}^D \omega_i = \Omega \end{aligned}$$

where $\{\omega_i\}_i^D$ are the eigenvalues of $\mathbb{E}_q[\nabla_{\mathbf{x}} \mathbf{f}^*(\mathbf{x}) \nabla_{\mathbf{x}} \mathbf{f}^*(\mathbf{x})^T]$, $\mathbf{f}^*(\mathbf{x}) = \mathbf{s}_p(\mathbf{x}) - \mathbf{s}_q(\mathbf{x})$ and $\sum_{\mathbf{r} \in O_{r_1}} \mathbf{r} \mathbf{r}^T = \mathbf{I}$ since $\mathbf{r} \in O_{r_1}$ are orthogonal to each other.

Thus, we can substitute it back, we have

$$S_{r_1, g_{r_1}} - S_{r_2, g_{r_2}} \geq \text{PSD}_{r_1} - \text{PSD}_{r_2} - C_{\text{sup}} \Omega$$

G.2. Proof of theorem 5

Proof. From proposition 4 we know $f_r^*(\mathbf{x}) = (s_p^r(x) - s_q^r(x))$, thus, we can substitute into PSD (Eq.7), we get

$$\text{PSD}_r = \max_{\mathbf{r} \in \mathbb{S}^{D-1}} \mathbb{E}_q \left[\left((s_p(\mathbf{x}) - s_q(\mathbf{x}))^T \mathbf{r} \right)^2 \right]$$

To maximize it, we consider the following constraint optimization problem.

$$\max_{\mathbf{r}} \mathbb{E}_q \left[\left((s_p(x) - s_q(x))^T \mathbf{r} \right)^2 \right] \quad \text{s.t.} \quad \|\mathbf{r}\|^2 = 1$$

We take the derivative of the corresponding Lagrange multiplier w.r.t. \mathbf{r} ,

$$\begin{aligned} & \mathbb{E}_q \left[\nabla_{\mathbf{r}} \left((s_p(\mathbf{x}) - s_q(\mathbf{x}))^T \mathbf{r} \right)^2 \right] - 2\lambda \mathbf{r} = 0 \\ & \Rightarrow \mathbb{E}_q \left[(s_p(\mathbf{x}) - s_q(\mathbf{x}))^T \mathbf{r} (s_p(\mathbf{x}) - s_q(\mathbf{x})) \right] = \lambda \mathbf{r} \\ & \Rightarrow \mathbb{E}_q \left[\underbrace{(s_p(\mathbf{x}) - s_q(\mathbf{x})) (s_p(\mathbf{x}) - s_q(\mathbf{x}))^T}_{\mathbf{S} = \mathbb{E}_q[\mathbf{f}^*(\mathbf{x}) \mathbf{f}^*(\mathbf{x})^T]} \right] \mathbf{r} = \lambda \mathbf{r} \\ & \Rightarrow \mathbf{S} \mathbf{r} = \lambda \mathbf{r} \end{aligned}$$

This exactly the problem of finding eigenpair for matrix \mathbf{S} . Let's assume $\mathbf{r} = \mathbf{v}$ which is the eigenvector of \mathbf{S} with corresponding eigenvalue λ . Substituting it back to PSD , we have

$$\begin{aligned} & \mathbb{E}_q \left[\left((s_p(\mathbf{x}) - s_q(\mathbf{x}))^T \mathbf{r} \right)^2 \right] \\ & = \mathbb{E}_q \left[(s_p(\mathbf{x}) - s_q(\mathbf{x}))^T \mathbf{r} (s_p(\mathbf{x}) - s_q(\mathbf{x})) \right]^T \mathbf{r} \\ & = \mathbf{r}^T \mathbf{S} \mathbf{r} \\ & = \lambda \mathbf{v}^T \mathbf{v} = \lambda \end{aligned}$$

Thus, to obtain the active slice \mathbf{r} , we only need to find the eigenvector of \mathbf{S} with the largest eigenvalue. \square

G.3. Greedy algorithm is eigen-decomposition

Corollary 6.2 (Greedy algorithm is eigen-decomposition). *Assume the conditions in theorem 5 are satisfied, then finding the orthogonal basis O_r from the greedy algorithm is equivalent to the eigen-decomposition of \mathbf{S} .*

Proof. Assume we have obtained the active slice \mathbf{r} from theorem 5, thus, we have $\mathbf{S} \mathbf{r} = \lambda \mathbf{r}$. The greedy algorithm for \mathbf{r}' can be translated into the following constrained optimization

$$\begin{aligned} & \max_{\mathbf{r}'} \mathbb{E}_q \left[\left((s_p(x) - s_q(x))^T \mathbf{r}' \right)^2 \right] \\ & \text{s.t.} \quad \|\mathbf{r}'\|^2 = 1 \\ & \quad \mathbf{r}'^T \mathbf{r}' = 0 \end{aligned}$$

By using Lagrange multipliers (μ, γ) , and then take derivative w.r.t. \mathbf{r}' ,

$$\mathbf{S} \mathbf{r}' = \mu \mathbf{r}' + \gamma \mathbf{r}$$

Then taking the inner product with \mathbf{r} in both side, and notice \mathbf{S} is a symmetric matrix, we obtain

$$\begin{aligned} \gamma & = \langle \mathbf{S} \mathbf{r}', \mathbf{r} \rangle \\ & = \langle \mathbf{r}', \mathbf{S}^T \mathbf{r} \rangle \\ & = \langle \mathbf{r}', \lambda \mathbf{r} \rangle = 0 \end{aligned}$$

Therefore, the constrained optimization is the same as the one in theorem 5, which is to find a eigenvector of \mathcal{S} that is different from \mathbf{r} . Repeat the above procedure, the final resulting O_r is a group of eigenvectors of \mathcal{S} . \square

H. Experiment Details

For all experiments in this paper, we use RBF kernel with median heuristics.

H.1. Benchmark GOF test

For gradient based optimization, we use Adam (Kingma & Ba, 2014) with learning rate 0.001 and $\beta = (0.9, 0.99)$. We use random initialization for SKSD-g+GO by drawing \mathbf{g}_r from a Gaussian distribution before normalizing them to unit vectors. For kernel smooth and gradient estimator, we use RBF kernel with median heuristics. Although the algorithm 1 states that small Gaussian noise are needed for active slices, in practice, we found that active slices still have the satisfactory performance without the noise.

The significance level for GOF test $\alpha = 0.05$, and the dimensions of the benchmark problems grow from 2 to 100. We use 1000 bootstrap samples to estimate the threshold and run 100 trials for each benchmark problems.

H.2. RBM GOF test

We set significance level $\alpha = 0.05$ and use 1000 bootstrap samples to compute the threshold. For methods that require training (SKSD based method), we need to collect some training samples. Following the same settings as (Gong et al., 2021), to avoid over-fitting to small training set, we collect the pseudo-samples during the early burn-in stage. Note that these pseudo-samples should not be used for testing, as they are not drawn from the q . We collect 2000 samples. For gradient based optimization, we use the same optimizer as benchmark GOF test with the same hyper-parameters. The batch size is 100. For initialization of SKSD+GO, we found that if the slices are initialized randomly, the gradient optimization fails to find meaningful slices within a reasonable amount of time, therefore, we have initialize the \mathbf{r} and \mathbf{g}_r as one-hot vectors and set $\mathbf{r} = \mathbf{g}_r$. For pruning ablation study, if the pruning level is set to 50, we initialize \mathbf{r} and \mathbf{g}_r to be the identity matrix. The default number of gradient optimization for SKSD+GO is 50. For active slice method, we directly use the active slices without any further optimizations. We run 100 trials for GOF test with 1000 test samples per trial.

(Gong et al., 2021) reports SKSD-rg+GO has near optimal test power at perturbation level 0.01. The performance difference is because they train the SKSD-rg with 200 batch sizes per burn-in step. Namely, the training set size are $200 \times 2000 = 400000$, which is 200 times larger than ours.

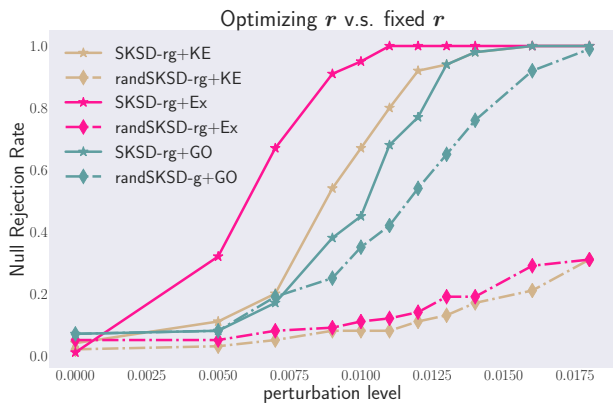


Figure 5. The test power difference with good \mathbf{r} and fixed \mathbf{r} .

They also run 2000 iterations, which is equivalent to 100 epochs in our settings.

Figure 5 shows the test power difference with optimized \mathbf{r} and fixed \mathbf{r} . The legend with *rand* annotation implies we randomly initialized \mathbf{r} as one-hot vectors and fix them while updating \mathbf{g}_r using GO or active slice. Without *rand*, it means both \mathbf{r} and \mathbf{g}_r are optimized. We only use 3 \mathbf{r} for active slice method and 50 for gradient-based counterpart. For active slice method with pruning (*randSKSD-g+Ex* or *randSKSD-g+KE*), despite we show that any finite random slices define a valid discrepancy, it is clear that the performance is quite poor with random initialized \mathbf{r} 's. It indicates that using active slices of \mathbf{g}_r alone cannot compensate the poor discriminating power of the random \mathbf{r} 's. Although SKSD-rg+GO demonstrates an advantage compared to randSKSD-g+GO, the performance boost is less clear compared to active slices method. This is because we do not use any pruning for randSKSD-g+GO, and adopt orthogonal basis $O_r = \mathbf{I}$. Despite the orthogonal basis may not capture the important directions, they can provide reasonable discriminating power due to their orthogonality from each other. In summary, using good directions for \mathbf{r} is advantageous compared to fixed \mathbf{r} .

H.3. Model learning: Training ICA

We use Adam optimizer for the model and slice directions with learning rate 0.001 and $\beta = (0.9, 0.99)$. We totally run 15000 iterations. The batch size is 100. We evaluate our method in dimension 10, 80, 100 and 150. For more stable comparisons, we initialized the weight matrix \mathbf{W} until its conditional number is smaller than its dimensions. For active slice method, we use randomly sampled 3000 data from training set to estimate the score difference and the matrices used for eigen-decomposition.

For SKSD-rg+GO, we initialize the \mathbf{r} to be a group of one-hot vectors to form identity matrix and $\mathbf{g}_r = \mathbf{r}$. We use an

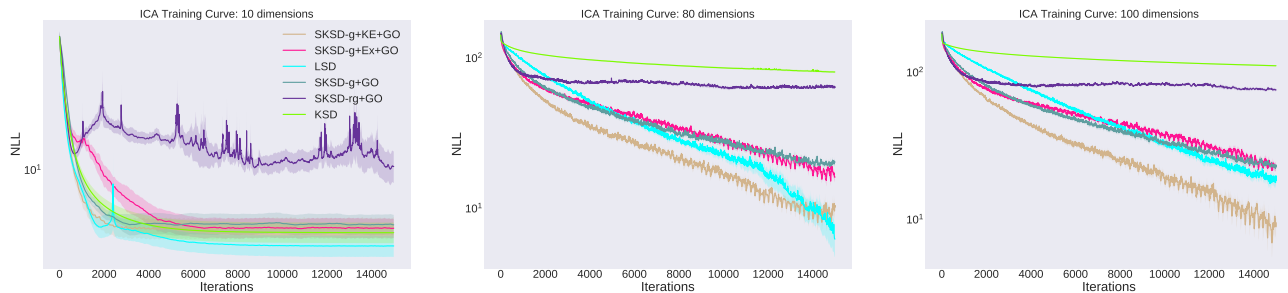


Figure 6. Training curve of ICA model with test NLL for different dimensions.

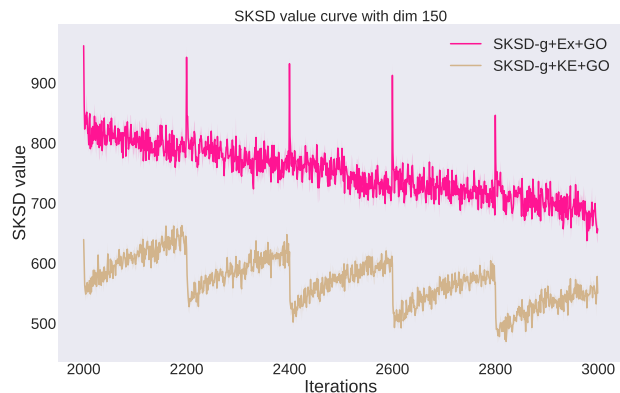


Figure 7. SKSD value curve with 150 dimensional ICA during iteration 5000 to 6000

adversarial training procedure that updates both r and g_r using Adam once per iteration before we update the model. For $SKSD-g+GO$, we fix the orthogonal basis O_r to be the identity matrix and only update g_r . Each results are the average of 5 runs of training.

As for the reason why $SKSD-g+Ex+GO$ performs worse than $+KE+GO$, we suspect that $+Ex$ only focus on directions with high discriminating power. However, high discriminating power is not necessarily good for model learning. It may focus on very small area that is different from the target but ignore the larger area with small difference. Because our algorithm for finding basis is greedy, this means it can ignore the generally good directions if they are not orthogonal to the directions with high discriminating power.

From figure 7, we can observe there is a spike of $SKSD-g+Ex+GO$ value at every 200 iterations due to the new active slices found at the beginning of each training epoch. However, the value drops significantly fast to the one before new active slices. This indicates the Ex indeed finds directions with large discriminating power but they do not represents good directions for learning due to the fast drop of SKSD values. On the other hand, the directions provided by KE does not give the highest discriminating power, but

it can find generally good directions of g_r using GO refinement steps within a few iterations. This means the directions found by KE indeed represents good directions for learning as the model cannot decrease this value quickly. We guess this is due to the smooth estimation of KE, where very small areas with high discriminating power are smoothed out.

Figure 6 shows the ICA training curve of other dimensions. We can observe the convergence speed of LSD deteriorates as the dimension increases due to the poor test function in early training stage, whereas $SKSD-g+KE+GO$ maintains the fastest convergence in high dimensions.